Steroidogenesis and androgen/estrogen signaling pathways are altered in *in vitro* matured testicular tissues of prepubertal mice

Short title: *In vitro* testicular steroidogenesis

Laura Moutard[1], Caroline Goudin[1], Catherine Jaeger[1], Céline Duparc[1], Estelle Louiset[1], Tony Pereira[2], François Fraissinet[2], Marion Delessard[1], Justine Saulnier[1], Aurélie Rives-Feraille[1], Christelle Delalande[3], Hervé Lefebvre[1], Nathalie Rives[1], Ludovic Dumont[1], Christine Rondanino[1*].

[1] Univ Rouen Normandie, Inserm, NorDic, UMR 1239, Adrenal and Gonadal Pathophysiology team, F-76000 Rouen, France

[2]Department of General Biochemistry, Rouen University Hospital, F-76000 Rouen, France

[3]Normandie Univ, UNICAEN, OeReCa, F-14000 Caen

* **Corresponding author**: christine.rondanino@univ-rouen.fr

Key words: androgen, estrogen, *in vitro* spermatogenesis, Leydig cell, mice, steroidogenesis

Abstract

Children undergoing cancer treatments are at risk for impaired fertility. Cryopreserved prepubertal testicular biopsies could theoretically be later matured *in vitro* to produce spermatozoa for assisted reproductive technology. A complete *in vitro* spermatogenesis has been obtained from mouse prepubertal testicular tissue, although with low efficiency. Steroid hormones being essential for the progression of spermatogenesis, the aim of this study was to investigate steroidogenesis and steroid signaling in organotypic cultures. Histological, RT-qPCR, western blot analyses and steroid hormone measurements were performed on *in vitro* cultured mouse prepubertal testicular tissues and age-matched *in vivo* controls. Despite a conserved density of Leydig cells after 30 days of culture (D30), transcript levels of adult Leydig cell and steroidogenic markers were decreased. Increased amounts of progesterone and estradiol and reduced androstenedione levels were observed at D30, together with decreased transcript levels of steroid metabolizing genes and steroid target genes. hCG was insufficient to facilitate Leydig cell differentiation, restore steroidogenesis and improve sperm yield. In conclusion, this study reports the failure of adult Leydig cell development and altered steroid production and signaling in tissue cultures. The organotypic culture system will need to be further improved before it can be translated in clinics for childhood cancer survivors.

Introduction

Pediatric cancer treatments such as chemotherapy have recognized toxicity on germline stem cells, which could lead to infertility at adulthood (1,2). Freezing of prepubertal testicular tissue containing spermatogonia is a fertility preservation option proposed to prepubertal boys with cancer prior to highly gonadotoxic treatments. Several fertility restoration approaches, whose aim is to mature cryopreserved tissues *in vivo* or *in vitro* in order to produce spermatozoa, are being developed. So far, these approaches have not been clinically validated. *In vitro* maturation strategies are currently being optimized in animal models. *In vitro* spermatogenesis could indeed be proposed to patients with testicular localization of residual tumor cells, for whom testicular tissue autografting is not indicated (about 30% of patients with acute leukemia). The organotypic culture procedure, which preserves testicular tissue architecture, microenvironment and cell interactions, has been used successfully to obtain spermatozoa from fresh or frozen/thawed mouse prepubertal testicular tissues (3–6). In addition, viable and fertile mouse offspring have been obtained from *in vitro* produced spermatozoa by oocyte microinjection (3,4).

It has been previously shown that supplementing organotypic culture media with retinol improves the *in vitro* production of spermatids and spermatozoa in prepubertal mouse testicular tissues cultured at a gas-liquid interphase (5,7). However, *in vitro* sperm production still remains a rare event. Transcript levels of the androgen receptor (AR)-regulated gene *Rhox5* were decreased at the end of the culture period, suggesting that testosterone production by Leydig cells and/or AR transcriptional activity could be impaired in organotypic cultures (8). A decline in intratesticular testosterone levels has been highlighted *in vitro* in 35- to 49-day cultures of 5 d*pp* mouse testes, i.e. after the end of the first wave of spermatogenesis (9). Moreover, our recent transcriptomic analysis reveals a decline in mRNA levels of *Cyp17a1*, encoding a steroidogenic enzyme, in 4- to 30-day cultures of 6 d*pp* mouse testes (10). Based

on these results, Leydig cell maturation and functionality need to be thoroughly explored in order to identify the molecular mechanism that are deregulated *in vitro*.

Two distinct populations of Leydig cells appear during mouse testicular development: (i) fetal Leydig cells arising during embryonic development and regressing over the first two weeks of postnatal life and (ii) adult Leydig cells appearing around one week after birth. Although they both express StAR (steroidogenic acute regulatory protein), CYP11A1 (P450 side chain cleavage), 3β-HSD1 (3β-hydroxysteroid dehydrogenase type 1) and CYP17A1 (P450 17α-hydroxylase/C17-20 lyase), which are steroidogenic proteins required for androgen production, 17β-HSD3 (17β-hydroxysteroid dehydrogenase type 3), which converts androstenedione to testosterone, is expressed only by adult Leydig cells (11,12). Consequently, the major androgens produced in fetal Leydig cells and adult Leydig cells are androstenedione and testosterone, respectively (13). In rodents, adult Leydig cells develop from undifferentiated stem Leydig cells through two intermediate cells, progenitor Leydig cells and immature Leydig cells (14). All these cells, except stem Leydig cells, express CYP11A1, 3β-HSD1 and CYP17A1 (15,16). 17β-HSD3 begins to be expressed in immature Leydig cells (17). The expression of the androgen metabolizing enzyme SRD5A1 (5α-reductase 1), which is high in progenitor and immature Leydig cells, is being silenced in adult Leydig cells (17). Adult Leydig cells express INSL3 (Insulin-like peptide 3) (18,19) as well as SULT1E1 (estrogen sulfotransferase) (12), which protects Leydig cells and seminiferous tubules against estrogen overstimulation by catalyzing the sulfoconjugation and inactivation of estrogens. Estrogens and androgens can also be inactivated in the testis by 17β-HSD2 (17β-hydroxysteroid dehydrogenase type 2), which converts estradiol to estrone and testosterone to androstenedione (20). Different factors, among which DHH (Desert hedgehog), IGF1 (Insulin-like Growth Factor 1) and LH (Luteinizing hormone) regulate the proliferation and differentiation of the Leydig cell lineage: DHH is required for both proliferation and

differentiation of stem Leydig cells (21), IGF1 stimulates the proliferation of progenitor Leydig cells and immature Leydig cells (22) and promotes the maturation of immature Leydig cells into adult Leydig cells (23), and LH is critical to both adult Leydig cell differentiation and their precursor proliferation (24).

The steroid hormones produced by Leydig cells are essential for the progression of spermatogenesis. Testosterone, synthesized under the control of LH, is essential for many aspects of spermatogenesis, including meiotic progression, spermiogenesis and germ cell survival (25–28). Androgen-binding protein (ABP), produced by Sertoli cells under the regulation of FSH, increases the accumulation of androgens in the seminiferous epithelium and makes them available for binding to intracellular AR (29). Estrogens, derived from the aromatization of androgens by CYP19A1 (aromatase) in somatic and germ cells, have been shown to be important for the long-term maintenance of spermatogenesis in the ArKO mouse (lacking aromatase) and for the progression of normal germ cell development in the ENERKI mouse (estrogen nonresponsive ERα knock-in) (30,31). The expression of aromatase is age-dependent, being mostly in Sertoli cells in immature rat testes and then in Leydig cells during adulthood (32,33). In mouse, aromatase is also present within seminiferous tubules, mainly in spermatids (34).

Androgens act directly on somatic cells (Sertoli cells and peritubular myoid cells) through AR to support germ cell development by regulating the expression of target genes. *Rhox5*, encoding a transcription factor that promotes germ cell survival (35), and *Eppin*, encoding a serine protease inhibitor, are target genes of testosterone in Sertoli cells, with androgen response elements (ARE) in their promoters (36). Several estrogen receptors mediate the effects of estrogens in the testis. In rodents, ERα was found in Leydig cells and peritubular myoid cells, ERβ was found in Sertoli cells and some germ cells (spermatogonia, spermatocytes) and GPER was detected in Leydig cells, Sertoli cells and germ cells

(spermatocytes, spermatids) (37–41). *Faah*, encoding a hydrolase that promotes Sertoli cell survival by degrading anandamide, is a direct target gene of estrogens in mature Sertoli cells (42,43). *Septin12*, containing 1 AR and 2 ERα binding sites in its promoter, has been identified as a potential novel target of the androgen and estrogen receptors in human testicular cells (44).

Since steroid hormones play an essential role in the progression of spermatogenesis, it appears necessary to ensure that their syntheses and mechanisms of action are not altered in *in vitro* cultured testicular tissues. The aim of the present work was therefore to study Leydig cell maturation, steroidogenesis and androgen/estrogen signaling in a comprehensive manner during the *in vitro* maturation of mouse prepubertal testicular tissues. The expression of Leydig cell markers, Leydig cell differentiation factors, steroidogenic enzymes, steroid receptors, steroid target genes and steroid contents were quantified in cultured tissues and in their *in vivo* counterparts. Although our organotypic culture conditions support a complete spermatogenesis, a failure of adult Leydig cell development with impaired steroidogenesis and altered steroid hormone signaling was demonstrated in this study.

Results

Leydig cells are partially mature after 30 days of organotypic culture

We first wondered whether Leydig cell number, survival, proliferation and differentiation could be altered under *in vitro* conditions. 3β-HSD immunofluorescence staining was performed to detect and quantify Leydig cells during mouse postnatal development and in *in vitro* cultured fresh testicular tissues (FT). The percentage of Leydig cells in apoptosis or in proliferation was measured after cleaved caspase 3 or Ki67 immunofluorescence staining respectively, and the percentage of Leydig cells expressing AR, which is required for their proliferation and maturation (51), was also determined. The transcript levels of genes

necessary for Leydig cell differentiation (*Igf1*, *Dhh*) and markers of fetal Leydig cells (*Mc2r*), progenitor/immature Leydig cells (*Srd5a1*) or adult Leydig cells (*Sult1e1*, *Insl3*) were then assessed by RT-qPCR. Finally, the concentration of INSL3, a marker of Leydig cell maturity, was measured by RIA in organotypic culture media and in testicular homogenates.

After 16 days of culture, the number of Leydig cells per cm² of testicular tissue was not significantly different from 22 d*pp*, the age-matched *in vivo* control (**Figure 1A-B**). However, at this time point, the percentage of apoptotic Leydig cells was increased compared to the *in vivo* control while the percentage of proliferating Leydig cells was unchanged (**Figure 1C-D**). In addition, the percentage of Leydig cells expressing AR was similar at D16 and 22 d*pp* (**Figure 1E**). Whereas no difference was observed in the mRNA levels of *Dhh*, *Srd5a1* and *Sult1e1* between D16 and 22 d*pp*, *Igf1* and *Insl3* transcripts levels were respectively higher and lower in 16-day organotypic cultures than *in vivo* (**Figure 1F-J**). *Mc2r* transcripts were barely detected at D16 and 22 d*pp* as well as at later time points, thereby reflecting the low amount of fetal Leydig cells in prepubertal testicular tissues (data not shown).

After 30 days of culture, no significant difference in the number of Leydig cells per cm² of testicular tissue and in the percentages of apoptotic and proliferating Leydig cells was observed compared to 36 d*pp*, the corresponding *in vivo* time point (**Figure 1A-D**). Furthermore, the percentage of Leydig cells expressing AR was comparable after *in vitro* or *in vivo* maturation (**Figure 1E**). The transcript levels of *Dhh* were also similar in *in vitro* and *in vivo* matured tissues at the end of the first spermatogenic wave (**Figure 1G**). However, a reduction in the mRNA levels of *Igf1*, *Srd5a1* and the two adult Leydig cell markers (*Sult1e1*, *Insl3*) was found at D30 in comparison to 36 d*pp* *in vivo* controls (**Figure 1F, H-J**). Moreover, intratesticular INSL3 was below the detection limit (<10 pg/mL) in *in vitro* matured tissues (**Figure 1K**) and a significant elevation in the concentration of INSL3 was observed in culture medium from D22 to D30 for FT tissues (**Figure 1L**).

In summary, while the number and proliferation of Leydig cells are not affected by organotypic culture conditions, their differentiation into mature adult Leydig cells is impaired *in vitro*.

Controlled slow freezing has no impact on Leydig cell density or state of differentiation before or after organotypic culture

In the clinics, testicular biopsies from prepubertal boys are frozen and stored in liquid nitrogen for later use. In order to assess the impact of freezing/thawing procedures (CSF) on Leydig cell number, survival, proliferation and differentiation in organotypic cultures, we conducted the same analyses as above on 6 d*pp* CSF mouse testicular tissues and on *in vitro* matured 6 d*pp* CSF tissues (**Figure 1** -figure supplement 1).

CSF had no impact on the number of Leydig cells per cm^2 of tissue at 6 d*pp* as well as after 16 or 30 days of culture (**Figure 1** -figure supplement 1**A-B**). Although the percentage of apoptotic Leydig cells was lower in CSF than in FT tissues at 6 d*pp*, it was similar in CSF and FT tissues at D16 and D30 (**Figure 1** -figure supplement 1**C**). Furthermore, no change in the percentage of Leydig cells in proliferation or expressing AR was found after CSF (**Figure 1** -figure supplement 1**D-E**). Moreover, *Dhh* and *Srd5a1* mRNA levels were similar in CSF and FT tissues (**Figure 1** -figure supplement 1**G-H**). *Igf1* transcript levels were decreased in CSF tissues at D16 (**Figure 1** -figure supplement 1**F**). Furthermore, *Sult1e1* mRNA levels were higher in CSF tissues at D30 (**Figure 1** -figure supplement 1**I**) and *Insl3* transcript levels were higher in CSF than in FT tissues at D16 and D30 (**Figure 1** -figure supplement 1**J**).

Since the number and the state of differentiation of Leydig cells are rather similar in FT and CSF tissues, it can be concluded that the freezing/thawing procedures are not harmful to these cells.

The expression of several actors of steroidogenesis is affected in organotypic cultures

As the differentiation of Leydig cells is not fully completed in organotypic cultures, we next wanted to know if actors of the steroidogenic pathway show deregulated expression *in vitro* in comparison to physiological conditions, and thus which steps of the steroid hormone biosynthesis pathway may be impaired. The transcript levels of several genes involved in steroidogenesis were measured by RT-qPCR to highlight a potential deregulation of their expression in cultured tissues (**Figure 2A-D, F, H-I**). The protein levels of two steroidogenic enzymes, 3β-HSD and CYP17A1, were also quantified by western blot (**Figure 2E, G**).

Controlled slow freezing had no impact on the mRNA levels of all the genes examined at 6 d*pp*, *i.e.* before culture (**Figure 2A-I**). At D16, the mRNA levels of *Star*, *Cyp17a1* and *Hsd17b3* were decreased in FT and CSF testicular tissues compared to 22 d*pp* testes (**Figure 2B, F, H**). *Cyp11a1* transcript levels were also lower in FT tissues at D16 than at 22 d*pp* (**Figure 2C**). In contrast, *Lhcgr*, *Hsd3b1* and *Hsd17b2* transcript levels remained unchanged at this time point (**Figure 2A, D, I**). 3β-HSD and CYP17A1 protein levels were not different between D16 and 22 d*pp* (**Figure 2E, G**).

The mRNA levels of *Cyp11a1*, *Hsd3b1*, *Cyp17a1* and *Hsd17b2* were lower at D30 in both FT and CSF tissues than in the physiological situation (**Figure 2C-D, F, I**). Despite a significant decrease in *Hsd3b1* mRNA levels at D30, the protein levels of 3β-HSD were not significantly different after 30 days of culture and at 36 d*pp* (**Figure 2E**). Western blot experiments however showed that the expression of CYP17A1 was also reduced at the protein level in both FT and CSF tissues at D30 compared to 36 d*pp* (**Figure 2G**). This steroidogenic enzyme was still detectable by immunofluorescence in Leydig cells in cultured tissues (**Figure 2J**). Finally, *Lhcgr* mRNA levels were found significantly reduced at D30 in FT tissues (**Figure 2A**), while *Star* and *Hsd17b3* mRNA levels were reduced at D30 in CSF tissues (**Figure 2B, H**).

Thus, the expression of several genes encoding steroidogenic enzymes is decreased *in vitro*, notably that of *Cyp17a1*, necessary for the conversion of progesterone to androstenedione.

Increased intratesticular concentrations of progesterone and estradiol combined with decreased intratesticular concentration of androstenedione in organotypic cultures

We then analyzed the steroid hormone content in *in vitro* cultured testicular tissues. The concentrations of androstenedione, DHEA and testosterone were measured by LC-MS/MS and the concentrations of progesterone and estradiol were assessed by ELISA in both testicular samples and the culture media (**Figure 3**). DHEA was below the detection limit (<1 ng/mL) in all the samples examined (data not shown). The intratesticular concentrations of progesterone were significantly increased at D16 and D30 in both FT and CSF tissues compared to their respective *in vivo* controls (**Figure 3A**). In contrast, the intratesticular concentrations of androstenedione were significantly decreased at D16 in both FT and CSF tissues and at D30 in FT tissues compared to *in vivo* controls (**Figure 3B**). The intratesticular concentrations of testosterone were however not different in *in vitro* and *in vivo* matured tissues at both time points (**Figure 3C**). In addition, the intratesticular concentrations of estradiol were significantly higher at D16 and D30 in FT and CSF tissues than in their respective *in vivo* controls (**Figure 3D**).

In the organotypic culture medium, a significant increase in the concentrations of progesterone was observed at D26 only (**Figure 3E**). Furthermore, a significant elevation in the concentrations of androstenedione was observed from D16 to D30 (**Figure 3E**). Regarding testosterone, following a decrease in the levels of this androgen in the culture media between D2 and D14, an augmentation was then detected between D26 and D30 (**Figure 3E**). At D30, the concentrations of both androstenedione and testosterone were higher in the culture media of FT tissues than of CSF tissues (**Figure 3** -figure supplement 1).

Regarding estradiol, no significant change in its concentrations was observed in the media between D6 and D30 (**Figure 3F**).

Since steroids are derived from cholesterol, intratesticular levels of total, free and esterified cholesterol were also analyzed (**Figure 3G**). The intratesticular levels of esterified cholesterol were comparable between the different experimental conditions (**Figure 3G**). However, total cholesterol levels were higher in FT and CSF cultured tissues at D16 and D30 compared to their corresponding *in vivo* time points (**Figure 3G**). Moreover, free cholesterol levels were increased in FT and CSF cultured tissues at D30 compared to 36 d*pp* and in FT tissues at D16 (**Figure 3G**).

Overall, our data show that the steroid content is altered in cultured testicular tissues, with an excess of free cholesterol, progesterone and estradiol and a deficiency of androstenedione.

Androgen and estrogen signaling are altered in 30-day organotypic cultures

The impact of imbalanced steroid hormone levels on downstream target gene expression was then investigated. The mRNA levels of actors of androgen and estrogen signaling were measured by RT-qPCR (**Figures 4 and 5**). The protein expression of the androgen receptor (AR), aromatase (CYP19) and fatty acid amide hydrolase (FAAH whose expression is regulated by estrogen) was also assessed by western blot (**Figures 4 and 5**).

The transcript levels of *Ar*, encoding the androgen receptor, were higher at D16 in FT tissues than at 22 d*pp* but were not significantly different between D30 and 36 d*pp* (**Figure 4A**). Conversely, AR protein levels were comparable at D16 in FT tissues and 22 d*pp* but were more elevated at D30 in both FT and CSF tissues than at 36 d*pp* (**Figure 4B**). Our immunofluorescence data showed that AR was expressed in Sertoli cells, peritubular myoid cells and Leydig cells in 16-day and 30-day cultured tissues as well as in the corresponding *in vivo* controls (**Figure 4C**). The transcript levels of two AR-regulated genes (*Rhox5*, *Eppin*)

and the AR/Erα-regulated gene *Septin12* were decreased in FT and CSF tissues cultured for 16 days compared to 22 d*pp* (**Figure 4D-F**). At D30, *Rhox5* and *Septin12* mRNA levels were still lower than *in vivo* while *Eppin* mRNA levels were higher than at 36 d*pp* (**Figure 4D-F**). In addition, a significant increase in *Abp* mRNA levels was found at D16 and D30 in CSF but not in FT tissues (**Figure 4G**).

Intriguingly, the expression of *Cyp19a1*, encoding aromatase, was drastically diminished after 30 days of culture in FT and CSF tissues compared to 36 d*pp* (**Figure 5A**). The protein levels of CYP19 were found reduced in both FT and CSF tissues at D16 and D30 (**Figure 5B**). CYP19 was expressed in Leydig cells at 6 d*pp* and was then found in elongated spermatids and spermatozoa at 36 d*pp*, whereas no expression could be detected in cultured testes (**Figure 5C**). CYP19 enzymatic activity was also significantly decreased in CSF cultures at D30 (**Figure 5D**). In addition, the transcript levels of the three genes encoding estrogen receptors (*Esr1*, *Esr2*, *Gper1*) and of the estrogen target gene *Faah* were significantly lower at D30 than at 36 d*pp* (**Figure 5E-H**). *Esr1* mRNA levels were also decreased at D16 (**Figure 5E**). FAAH protein levels were decreased in 16-day FT and 30-day CSF organotypic cultures (**Figure 5I**).

Thus, the expression of many genes in the androgen and estrogen signaling pathways are deregulated under organotypic culture conditions.

hCG is insufficient to stimulate Leydig cell differentiation and to restore steroidogenesis and steroid hormone signaling

As LH is known to stimulate the differentiation of the adult Leydig cell lineage and steroidogenesis, we wondered whether supplementation of organotypic culture media with hCG (LH homolog) could restore steroidogenesis to control levels. In order to determine the dose to be used, we examined the impact of different hCG concentrations (5 pM, 50 pM, 1 nM, 5 nM or 50 nM) on the intratesticular concentrations of testosterone and the secretion of

this hormone in the organotypic culture medium. Since the concentration of hCG leading to the best response (*i.e.* plateau of the dose-response curves for intratesticular and secreted testosterone) was 1 nM, we used this dose for the rest of the analyses (**Figure 6** -figure supplement 1).

Upon supplementation with 1 nM hCG, intratesticular androstenedione levels were significantly increased at D30 in FT but not CSF tissues (**Figure 6A**). The intratesticular testosterone levels were higher at D30 in both FT and CSF tissues following hCG supplementation (**Figure 6B**). Moreover, a significant increase in androstenedione and testosterone concentrations was observed in the culture media of both FT and CSF tissues following hCG supplementation (**Figure 6C-D**). The amounts of androgens released into the culture media were however lower for CSF tissues than for FT tissues (**Figure 6C-D**).

The addition of 1 nM hCG had no impact on the transcript levels of *Star*, *Hsd17b3*, *Hsd3b1*, *Ar* and *Esr1* in both FT and CSF cultures (**Figure 6F, I, J, L, P**). *Hsd17b3* and *Esr1* mRNA levels still remained lower upon hCG supplementation than *in vivo* (**Figure 6I, P**). No effect of hCG was also observed in FT cultures for *Cyp17a1*, *Faah*, *Srd5a1*, *Sult1e1*, *Insl3*, *Igf1*, *Dhh*, *Abp* and *Hsd17b2* mRNA levels (**Figure 6I, J, S, Figure 6** -figure supplement 2). *Lhcgr*, *Cyp11a1*, *Cyp19a1*, *Esr2* and *Gper1* mRNA levels were increased after hCG supplementation in FT cultures (**Figure 6E, G-H, K, Q, R**). Whereas *Cyp11a1* and *Cyp19a1* mRNA levels were still lower after hCG supplementation than *in vivo* **(Figure 6G, K)**, *Esr2* and *Gper1* transcripts were restored to their physiological levels (**Figure 6Q-R**). In contrast, mRNA levels of *Rhox5*, *Eppin*, *Septin12* and *Igf1* were decreased after hCG supplementation in FT cultures, with *Rhox5* and *Septin12* transcript levels lower than those observed *in vivo* (**Figure 6M-O**).

Finally, the mean proportions of seminiferous tubules reaching the round spermatid and elongated spermatid stages were lower in tissues cultured with than without hCG (**Figure**

6T). The number of Sertoli cells inside seminiferous tubules was unchanged following hCG supplementation, but was higher than in *in vivo* controls (**Figure 6U**).

Although the addition of hCG resulted in increased androgen levels, the expression of adult Leydig cell markers, of several steroidogenic genes and of steroid hormone-regulated genes remained low, thus not promoting the progression of *in vitro* spermatogenesis.

Discussion

The present study shows for the first time and in a comprehensive manner that Leydig cell maturation and functionality as well as steroid hormone signaling are impaired in cultures of fresh and frozen/thawed immature mouse testes. Only few differences were found between fresh and frozen/thawed *in vitro* matured tissues.

A similar density of Leydig cells was found in organotypic cultures and in corresponding *in vivo* controls. However, Leydig cells only partially matured *in vitro*. At D16, the expression of the Leydig cell differentiation factors *Igf1* and *Dhh* was unaffected. At D30, the proliferation/apoptosis balance was undisturbed in Leydig cells while the expression of *Insl3* was faint, as well as that of *Sult1e1*, another Leydig cell maturity marker. The deficient Leydig cell maturation observed at D30 could be related to the decreased levels of *Igf1*, which encodes insulin-like growth factor 1 known to promote the maturation of immature Leydig cells into adult Leydig cells (23).

Leydig cell functionality was also altered in organotypic cultures. Indeed, the expression of several genes encoding steroidogenic enzymes (*Cyp11a1*, *Cyp17a1*, *Hsd17b3*, *Hsd17b2*) was downregulated in these cells (**Figure 7**). Reduced *Cyp17a1* mRNA levels in organotypic cultures were also recently highlighted using a bulk RNA-seq approach (10). Decreased *Cyp11a1* and *Cyp17a1* transcript levels were previously reported in *Igf1*$^{-/-}$ mice, together with decreased intratesticular testosterone levels (22). Furthermore, deficiency in insulin-like growth factors signaling in *Insr*$^{-/-}$/*Igf1r*$^{-/-}$ mouse Leydig cells was shown to impair testicular

steroidogenesis (decreased *Lhcgr*, *Star*, *Cyp11a1*, *Cyp17a1*, *Hsd17b3*, *Srd5a1* and *Insl3* mRNA levels) and increase estradiol production (52). Here, we report for the first time an accumulation of estradiol in *in vitro* cultured tissues, which could be deleterious for sperm production. To promote Leydig cell maturation and lower intratesticular estradiol levels *in vitro*, supplementation of culture medium with IGF1 could thus be later envisaged, and even more so since this factor has been shown to increase, although modestly, the percentages of round and elongated spermatids in cultured mouse testicular fragments (53). To reduce estrogen levels and increase sperm production, supplementation of the organotypic culture medium with selective estrogen receptor modulators such as tamoxifen or with aromatase inhibitors such as letrozole could also be considered in future studies. These molecules have indeed proven to be effective in increasing sperm concentration in infertile men (54–56).

Our work also revealed an elevation in progesterone and a reduction in androstenedione in *in vitro* matured tissues (**Figure 7**), which could arise from the reduced expression of *Cyp17a1*. A greater sperm production has been highlighted in PRKO mice (lacking the progesterone receptor), thereby showing the inhibitory action of progesterone on spermatogenesis (57). The cumulative excess of progesterone and estradiol in cultured testicular tissues may therefore slow the progression of *in vitro* spermatogenesis and lead to a poor sperm yield.

Despite the disturbed steroidogenic activity of Leydig cells *in vitro*, the accumulation of estradiol and progesterone, the decrease in androstenedione, and in contradiction with a previous study (9), intratesticular testosterone levels in cultured tissues were not significantly different from *in vivo*. Moreover, a complete *in vitro* spermatogenesis was achieved, albeit with a low efficiency as previously described (5,6). We also found that the percentage of Leydig cells expressing AR was unchanged under *in vitro* conditions. The increased AR protein levels at D30 could thus be the result of the higher number of Sertoli cells within

seminiferous tubules. Intriguingly, common points can be observed in our organotypic cultures and in LCARKO (Leydig cell-specific *Ar*$^{-/-}$) mice (58): decreased *Insl3*, *Cyp17a1* and *Hsd17b3* mRNA levels, increased intratesticular progesterone levels and unchanged intratesticular testosterone levels compared to controls. This could suggest that AR signaling is dysfunctional in Leydig cells *in vitro*. The downregulation of *Rhox5* expression (**Figure 7**), which confirms our previous findings (8), further suggests that AR signaling may also be impaired in Sertoli cells. Recently, in a mouse model with disrupted dimerization of the AR ligand-binding-domain, a decreased expression of *Hsd17b3* and of AR-regulated genes, such as *Rhox5* and *Insl3*, a higher percentage of Sertoli cells and a decreased production of round and elongated spermatids were found (59), which further supports our hypothesis that AR signaling may be defective in organotypic cultures. In the SPARKI (SPecificity-affecting AR KnockIn)-AR mouse model, which has a defect in binding to AR-specific DNA motifs while displaying normal interaction with the classical AREs, it has been shown that *Rhox5* expression is regulated by an AR-selective ARE, while *Eppin* expression is regulated by a classical, nonselective ARE (60). The differential regulation of these two androgen-responsive genes could explain why *Rhox5* mRNA levels were downregulated while *Eppin* mRNA levels were upregulated in our cultures. We also report here that the transcript levels of *Septin12*, a potential target of the androgen and estrogen receptors, was reduced *in vitro* (**Figure 7**).

Additionally, estrogen signaling was impaired in organotypic cultures, with a low expression of the estrogen-synthesizing enzyme aromatase, of estrogen receptors and of the estrogen target gene *Faah* (**Figure 7**). Since the expression of *Cyp19a1*, *Esr1* and *Esr2* (encoding aromatase, ERα and ERβ, respectively) can be downregulated by estradiol in the rat testis (61,62), we hypothesize that the transcription of these genes may be negatively controlled by elevated estradiol levels in our tissue cultures. *Faah*, whose promoter activity engages ERβ

and the histone demethylase LSD1, is a direct target gene of estrogens in Sertoli cells (42). The *Faah* proximal promoter is not regulated by estrogen in immature Sertoli cells, as they express ERβ at the same level as mature cells but do not express LSD1 (42). Thus, the decreased *Faah* transcript levels in organotypic cultures could be the consequence of the downregulated ERβ expression and/or of the immaturity of Sertoli cells. Whether Sertoli cells in organotypic cultures are as mature as *in vivo* is unknown and will be the focus of future studies. The transcription of *Insl3*, which is repressed by estradiol in a MA-10 Leydig cell line model (63), could also be inhibited by the excess of estradiol in our tissue cultures. Interestingly, our *in vitro* cultured testes exhibit common features with the testes of *Sult1e1*$^{-/-}$ mice lacking estrogen sulfotransferase, an enzyme that catalyzes the sulfoconjugation and inactivation of estrogens (64): decreased *Cyp17a1* expression as well as increased progesterone levels and local estrogen activity (65,66). In organotypic cultures, estrogen excess could be explained by low *Sult1e1* expression. In addition, reduced transcript levels of *Hsd17b2*, encoding an enzyme that converts estradiol to estrone and testosterone to androstenedione, may also explain why estradiol levels remain elevated in cultures while testosterone levels are similar to controls and androstenedione levels are low.

Finally, as previously reported (5,6), the presence of LH or its homolog hCG was not necessary to reconstitute a full first spermatogenic wave *in vitro*. However, plasma LH concentration is known to rise *in vivo* from 21-28 d*pp* in the mouse model (67). We previously showed that the addition of 0.075 nM (50 IU/L) hCG together with FSH from D7 onwards modestly increased the number of spermatozoa produced in organotypic cultures (5). To mimic as closely as possible the physiological conditions, 1 nM hCG was added in the culture medium from D16 onwards. Even though Leydig cells responded to this stimulation by synthesizing and secreting more androgens, supplementation of the culture medium with 1 nM hCG alone was not sufficient to facilitate Leydig cell differentiation, restore

steroidogenesis and steroid hormone signaling and increase the yield of *in vitro* spermatogenesis.

In conclusion, the present study shows the partial maturation and the disturbed steroidogenic activity of Leydig cells, the abnormal steroid hormone content as well as the altered androgen and estrogen signaling in organotypic cultures of fresh and frozen/thawed prepubertal mouse testicular tissues. Altogether, these defects could contribute to the low efficiency of *in vitro* spermatogenesis. It will therefore be necessary to optimize the culture medium by adding factors that promote proper Leydig cell differentiation as well as the culture design to prevent central necrosis from affecting the survival and/or the growth and/or the differentiation of the testis in culture. The development of an optimal model of *in vitro* spermatogenesis could be useful in advancing the field of fertility restoration, but could also have wider applications, as it could be useful for studying the initiation of puberty as well as the impact of cancer therapies, drugs, chemicals and environmental agents (e.g. endocrine disruptors) on the developing testis.

Materials and methods

Key resources table

Key Resources Table				
Reagent type (species) or resource	**Designation**	**Source or reference**	**Identifiers**	**Additional information**
biological sample (*Mus musculus*, male)	Testis	CD-1 Mice from Charles River		Freshly isolated from male *Mus musculus* (CD-1)

antibody	Anti-3β-HSD (mouse monoclonal)	Santa Cruz Biot.	sc-515120 (AF488)	IF (1:100), WB (1:1000)
antibody	Anti-β-Actin (mouse monoclonal)	Abcam	ab8226	WB (1:5000)
antibody	Anti-AR (rabbit monoclonal)	Abcam	ab133273	IF (1:100), WB (1:5000)
antibody	Anti-CC3 (rabbit polyclonal)	Abcam	ab49822	IF (1:200)
antibody	Anti-CYP17A1 (rabbit polyclonal)	Abcam	ab231794	IF (1:200), WB (1:10000)
antibody	Anti-CYP19A1 (mouse monoclonal)	BioRad	MCA2077 S	IHC (1:50), WB (1:250)
antibody	Anti-FAAH (rabbit polyclonal)	Proteintech	17909-1-AP	WB (1:1000)
antibody	Anti-Ki67 (rabbit monoclonal)	Abcam	ab16667	IF (1:100)
antibody	Anti-mouse Alexa 488 (goat)	Abcam	ab150113	IF (1:200)
antibody	Anti-rabbit Alexa 488 (goat)	Abcam	ab150077	IF (1:200)
antibody	Anti-rabbit Alexa 594 (goat)	Abcam	ab150080	IF (1:200)
antibody	Anti-mouse HRP (goat)	Invitrogen	31430	WB (1:5000)
antibody	Anti-rabbit HRP (goat)	Invitrogen	A16110	WB (1:5000)
commercial assay or kit	RNeasy Micro kit	Qiagen	74004	

commercial assay or kit	qScript cDNA SuperMix	QuantaBio	95048	
commercial assay or kit	Lipid Extraction kit	Abcam	ab211044	
commercial assay or kit	Cholesterol/Cholesteryl Ester assay kit	Abcam	ab65359	
commercial assay or kit	Progesterone ELISA kit	Cayman Chemical Company	582601	
commercial assay or kit	Estradiol ELISA kit	Cayman Chemical Company	501890	
commercial assay or kit	Aromatase (CYP19A) Activity assay kit	Abcam	ab273306	
commercial assay or kit	INSL3 RIA kit	Phoenix Pharmaceuticals	RK-035-27	
chemical compound, drug	KSR	Gibco by Life Technologies	10828010	(10%)
chemical compound, drug	Retinol	Sigma-Aldrich	R7632	1 µM
chemical compound, drug	hCG	MSD France	Ovitrelle	1 nM
chemical compound, drug	SYBR Green	Thermo Fisher Scientific	4385616	

Ethical approval

All the experimental procedures were approved by the Institutional Animal Care and Use Committee of Rouen Normandy University under the licence/protocol number APAFiS #38239.

Mice and testis collection

CD-1 mice (Charles River Laboratories, L'Arbresle, France) were housed in a temperature-controlled room (22–23°C) under a 12-h light/dark cycle. Prepubertal 6-day *postpartum* (d*pp*) male mice were euthanized by decapitation and underwent a bilateral orchiectomy. Testes were transferred to Petri dishes containing α-MEM without phenol red (Gibco by Life Technologies, Saint-Aubin, France) and the complete removal of the tunica albuginea was performed with two needles under a binocular magnifier (S8AP0, Leica Microsystems GmbH, Wetzlar, Germany). Testes were then either cultured immediately (culture from fresh tissues), or after a freezing/thawing cycle (**Figure 8**). Moreover, mice aged 22 and 36 d*pp* were euthanized by CO_2 asphyxiation and their testes were used as *in vivo* controls for 16 and 30 days of culture, respectively (**Figure 8**).

Controlled slow freezing (CSF) and thawing of testicular tissues

Freezing procedure

Testes were placed into cryovials (Dominique Dutscher, Brumath, France) containing 1.5 mL of the following cryoprotective medium: Leibovitz L15 medium (Eurobio, Courtabœuf, France) supplemented with 1.5 M dimethylsulfoxyde (DMSO, Sigma-Aldrich, Saint-Quentin Fallavier, France), 0.05 M sucrose (Sigma-Aldrich), 10% (v/v) fetal calf serum (FCS, Life Technologies) and 3.4 mM vitamin E (Sigma-Aldrich) (45). After a 30-min equilibration at 4°C, samples were frozen in a programmable freezer (Nano Digitcool, CryoBioSystem, L'Aigle, France) with a CSF protocol: start at 5°C, then -2°C/min until reaching -9°C, stabilization at -9°C for 7 min, then -0.3°C/min until -40°C and -10°C/min down to -140°C. Testicular tissues were then plunged and stored in liquid nitrogen.

Thawing procedure

Cryotubes were warmed for 1 min at room temperature (RT) and then for 3 min in a water bath at 30°C. They were then successively incubated at 4°C in solutions containing decreasing

concentrations of cryoprotectants for 5 min each [solution 1: 1 M DMSO, 0.05 M sucrose, 10% FCS, 3.4 mM vitamin E, Leibovitz L15; solution 2: 0.5 M DMSO, 0.05 M sucrose, 10% FCS, 3.4 mM vitamin E, Leibovitz L15; solution 3: 0.05 M sucrose, 10% FCS, 3.4 mM vitamin E, Leibovitz L15; solution 4: 10% FCS, 3.4 mM vitamin E, Leibovitz L15].

Organotypic cultures at a gas–liquid interphase

In vitro tissue cultures were performed as previously described (3,5). Briefly, prepubertal 6-day old mouse testes, which contain spermatogonia as the most advanced type of germ cells, were first cut into four fragments (approximately 0.75 mm^3 each, which was previously determined to be the most appropriate size for mouse *in vitro* spermatogenesis) (7). They were placed on top of two 1.5% (w/v) agarose Type I gels (Sigma-Aldrich) half-soaked in medium. Testicular tissues were then cultured under 5% CO_2 at 34°C for 16 days (D16), which corresponds to the end of meiosis and the appearance of the first round spermatids, or 30 days (D30) to explore the end of the first spermatogenic wave. No growth of the fragments was observed during the organotypic culture period (Figure 8-figure supplement 1A). The basal medium (BM) contained α-MEM without phenol red, 10% KSR (KnockOut Serum Replacement, Gibco by Life Technologies), 0.1 mg/mL streptomycin and 100 UI/mL penicillin (Sigma-Aldrich). The medium was chosen without phenol red because of its estrogen activity (46). Retinol (10^{-6} M, Sigma-Aldrich) was added in all organotypic cultures from D2 and then every 8 days in order to respect the meiosis entry cycle of spermatogonia (5). Furthermore, the basal medium was supplemented or not with 1 nM hCG (human Chorionic Gonadotropin, MSD France, Courbevoie, France) from D16 in order to stimulate Leydig cell differentiation and assess Leydig cell functionality. Media were prepared just before use and were replaced twice a week.

Histological analyses

Tissue fixation, processing and sectioning

Testicular tissues were fixed with Bouin's solution (Sigma-Aldrich) or 4% paraformaldehyde (PFA, Sigma-Aldrich) for 2 h at room temperature. They were then dehydrated in ethanol in the Citadel 2000 tissue processor (Shandon, Cheshire, UK) and embedded in paraffin. Tissue sections (3 µm thick) were prepared with the RM2125 RTS microtome (Leica) and were mounted on Polysine slides (Thermo Fisher Scientific, Waltham, MA, USA).

Periodic Acid Schiff (PAS) reaction

A PAS reaction was then performed on *in vitro* matured tissues. Tissue sections were deparaffinized in xylene and rehydrated in decreasing concentrations of ethanol. Slides were then immersed in 0.5% periodic acid (Thermo Fisher Scientific) for 10 min, rinsed for 5 min in water and then placed for 30 min in the Schiff reagent (Merck, Darmstadt, Germany). After three 2-min washes in water, sections were counterstained with Mayer's hematoxylin and mounted with Eukitt (CML, Nemours, France). Images were acquired on a DM4000B microscope (Leica) at a ×400 magnification. The most advanced type of germ cells present in the testicular fragments was analyzed in at least 30 cross-sectioned seminiferous tubules (located at the periphery of the cultured fragments, i.e. outside of the necrotic region) (Figure 8-figure supplement 1E-F) from 2 sections with the Application Suite Core v2.4 software (Leica).

Immunofluorescence staining

After deparaffinization, rehydration and a 3-min wash in phosphate buffered saline (PBS, Sigma-Aldrich), tissue sections were boiled in 10 mM citrate buffer pH 6.0 (Diapath, Martinengo, Italy) for 40 min at 96°C. They were cooled for 20 min at RT and rinsed in distilled water for 5 min. A permeabilization step with 0.1% (v/v) Triton X-100 (Sigma-Aldrich) was performed at RT for 15 min for Ki67/3β-HSD immunostaining. Non-specific sites were blocked with 5% (w/v) bovine serum albumin (BSA, Sigma-Aldrich) and 5% (v/v) horse serum (Sigma-Aldrich). Slides were then incubated in humidified environment with

primary antibodies (**Supplementary File 1a**), rinsed 3 times in PBST (PBS with 0.05% Tween-20) and incubated with appropriate secondary antibodies (**Supplementary File 1a**). For Ki67/3β-HSD, a sequential protocol was performed as follows: incubation with anti-Ki67 antibodies overnight at 4°C, incubation with secondary antibodies coupled to Alexa 594 for 60 min at RT, fixation with 4% PFA for 15 min at RT and incubation with anti-3β-HSD antibodies directly coupled to Alexa 488 for 90 min at RT. Negative controls were carried out by omitting the primary antibodies. Sections were washed, dehydrated with ethanol and mounted in Vectashield with Hoechst. Images were acquired on a THUNDER Imager 3D Tissue microscope (Leica) at a ×400 magnification. Leydig cell number (3β-HSD^{+}) was normalized to tissue area (cm²).

Immunohistochemical staining

After deparaffinization and rehydration, endogenous peroxidases were blocked with HP Block (Dako, Les Ulis, France) for 30 min and non-specific binding sites were blocked with Ultra-V Block solution (Thermo Fisher Scientific) for 10 min at RT. Tissue sections were then incubated overnight at 4°C with anti-CYP19A1 antibodies (**Supplementary File 1a**). After three 5-min washes in PBS, they were incubated for 10 min at RT with biotinylated polyvalent secondary antibodies (UltraVision Detection System HRP kit, Thermo Fisher Scientific). After three 5-min washes in PBS, a 10-min incubation at RT with streptavidin associated with peroxidase (UltraVision Detection System HRP kit, Thermo Fisher Scientific) was performed. The labeling was revealed after application of a chromogenic substrate (EnVision FLEX HRP Magenta Chromogen, Dako) for 10 min at RT. A negative control was carried out by omitting the primary antibody.

RNA extraction and RT-qPCR

RNA extraction

Total RNA was extracted from testicular samples using RNeasy Micro kit (Qiagen, Courtabœuf, France) according to the manufacturer's instructions. For *in vitro* cultured tissues, the central necrotic area (16-27% of the explants, Figure 8-figure supplement 1B-F) was carefully removed before RNA extraction, so that transcript levels in the healthy part of the samples (i.e. where *in vitro* spermatogenesis occurs) could be measured and compared with *in vivo* controls. To avoid contamination with genomic DNA, extracted RNA was incubated with two units of TURBO DNase (Life Technologies) for 45 min at 37°C. The amount of the RNA samples was measured with a NanoDrop Spectrophotometer (NanoDrop Technologies, Wilmington, DE, USA) and purity was determined by calculating the ratio of optical densities at 260 nm and 280 nm.

Reverse transcription

The reverse transcription reaction was performed in a 96-well plate from 1 µg total RNA with 4 µL of qScript cDNA SuperMix 5X (QuantaBio, Gaithersburg, MD, USA) and ribonuclease-free water to adjust the volume to 20 µL. Reverse transcription was performed according to the following program: 5 min at 25°C, 30 min at 42°C and 5 min at 85°C. The complementary DNA (cDNA) obtained were diluted 1:10.

Polymerase chain reaction

cDNA amplifications were carried out in a total volume of 13 µL containing 6 ng of cDNA templates, 6.5 µL of SYBR Green (Thermo Fisher Scientific) and 300 nM of each primer. Specific primers are listed in **Supplementary File 1b**. Samples were dispensed using the Bravo pipetting robot (Agilent Technologies, Santa Clara, CA, USA). Reactions were performed in 384-well plates (Life Technologies) in a Quant Studio 12K Flex system. The amplification condition was 20 s at 95°C followed by 40 cycles (1 s at 95°C, 20 s at 60°C) and a final step of denaturation of 15 s at 95°C, 1 min at 60°C and 15 s at 95°C. Melting curves were obtained to ensure the specificity of PCR amplifications. The size of the

amplicons was verified by agarose gel electrophoresis (E-gel 4%, Life Technologies). The relative expression level of each gene was normalized to two housekeeping genes as recommended by the MIQE guidelines (47): *Gapdh* and *Actb*, which were identified and validated as the most stable and suitable genes for RT-qPCR analysis in mouse testis development (48). 3β-hydroxysteroid dehydrogenase (*Hsd3b1*), a selective Leydig cell marker, has been used as a normalization factor for the analysis of genes expressed in Leydig cells (49). Data were analyzed using the $2^{-\Delta\Delta Ct}$ method (50).

Western blot

Protein extraction

Testes were homogenized in ice-cold RIPA buffer (50 mM Tris HCl, 0.5% cholic acid, 0.1% SDS, 150 mM NaCl) containing a protease inhibitor cocktail (Sigma-Aldrich). For *in vitro* cultured tissues, the central necrotic area was carefully removed before protein extraction.

Determination of protein concentration by the Bradford method

Total protein concentration was measured in the homogenates. The assay was performed in a 96-well plate in a final volume of 200 µL containing the sample and Bradford's solution (BioRad, Marnes-la-Coquette, France). After a 5-min incubation at RT, the optical density at 595 nm was measured using a Spark spectrophotometer (Tecan, Lyon, France).

Western blot

Protein extracts (20 µg) were separated on 12% resolving polyacrylamide gels (BioRad) and transferred onto nitrocellulose membranes (BioRad). The membranes were blocked with 5% milk or 5% BSA in TBST (0.2% Tween-20 in Tris Buffered Saline) for 30 min at 37°C before incubation overnight at 4°C with the appropriate primary antibody (**S1 Table**). After washes, membranes were incubated with the appropriate HRP-conjugated secondary antibodies (**S1 Table**). ECL reagents (BioRad) were used to detect the immunoreactivity. Images were captured with the ChemiDoc XRS+ Imaging System (BioRad). Densitometric analyses were

performed using Image Lab™ v5.0 software (BioRad) and protein levels were normalized to β-actin or to the Leydig cell-specific marker 3β-HSD.

Intratesticular cholesterol levels

Total testicular lipids were extracted from ~10 mg tissue with a Lipid Extraction kit (ab211044; Abcam, Paris, France) according to the manufacturer's instructions. Dried lipid extracts were reconstituted in 200 µL of assay buffer. Intratesticular levels of total, free, and esterified cholesterol were measured with a colorimetric Cholesterol/Cholesteryl Ester assay kit (ab65359; Abcam) according to the manufacturer's instructions.

Hormonal assays

Sample preparation for liquid chromatography coupled to mass spectrometry (LC-MS/MS)

Testicular fragments were homogenized in 200 µL (6 d*pp* tissues and *in vitro* matured tissues) or 400 µL (22 d*pp* and 36 d*pp* tissues) of 0.1 M phosphate buffer pH 7.4 with a cocktail of protease inhibitors (Sigma-Aldrich). Total protein concentration was measured as described above.

LC-MS/MS

The standards for androstenedione, testosterone, dehydroepiandrosterone (DHEA) and their stable labeled isotopes were obtained from Merck. Working solutions were prepared in methanol. Serial dilutions from working solutions were used to prepare seven-point calibration curves and 3 quality control levels for all analytes. For the final calibration and quality control solutions, PBS was used for testicular fragments and α-MEM for medium. The linearity ranges were from 0.05 to 10 ng/mL for androstenedione and testosterone, and from 1 to 200 ng/mL for DHEA. A simple deproteinization was carried out by automated sample preparation system, the CLAM-2030 (Shimadzu Corporation, Marne-la-Vallée, France) coupled to a 2D-UHPLC-MS/MS system. Once the sample on board, 30 µL was

automatically pipetted in a pre-conditioned tube containing a filter, in which reagents were added, then mixed and filtered. Briefly, the polytetrafluoroethylene (PTFE) filter vial (0.45 µm pore size) was previously conditioned with 20 µL of methanol (Carlo Erba, Val-de-Reuil, France). Successively, 30 µL of sample and 60 µL of a mixture of isotopically labeled internal standards in acetonitrile were added. The mixture was agitated for 120 s (1900 rpm), then filtered by application of vacuum pressure (-60 to -65 kPa) for 120 s into a collection vial. Finally, 30 µL of the extract was injected in the 2D-UHPLC-MS/MS system.

Analysis was performed on a two dimensions ultra-performance liquid chromatograph-tandem mass spectrometer (2D-UHPLC-MS/MS) consisting of the following Shimadzu® modules (Shimadzu Corporation): an isocratic pump LC20AD SP, for pre-treatment mode, a binary pump consisting of coupling two isocratic pumps Nexera LC30AD for the analytical mode, an automated sampler SIL-30AC, a column oven CTO-20AC and a triple-quadrupole mass spectrometer LCMS-8060. The assay was broken down into two stages. The first was the pre-treatment where the sample was loaded on the perfusion column. The second step was the elution of the compounds of interest to the analytical column. The deproteinized extract performed by the CLAM-2030 was automatically transferred to the automated sampler, where 30 µL was directly analyzed into the chromatographic system. The LC-integrated online sample clean-up was performed using a perfusion column Shimadzu® MAYI-ODS (5 mm L × 2 mm I.D.). The first step consisted of loading the extract on the perfusion column with a mobile phase composed of 10 mM ammonium formate in water (Carlo Erba) at a flow rate of 0.5 mL/min during 2 min. Then the system switched to the analytical step to elute the analytes from the perfusion column to the analytical column to achieve chromatographic separation. During this step, the loading line was washed with propan-2-ol (Carlo Erba) during 3 min. Chromatographic separation was achieved on a Restek® Raptor Biphenyl (50 mm L × 3 mm I.D. , 2.7 µm) maintained at 40 °C and a gradient of (A) 1 mM ammonium fluoride buffer in

water (Carlo Erba) and (B) methanol (Carlo Erba) at a flow rate of 0.675 mL/min as follows: 0.0–2.10 min, 5% (B); 2.1–3.0 min, 5 to 65% (B); 3.0–4.75 min, 65% (B); 4.75–5.0 min, 65 to 70% (B); 5.0–6.6 min, 70% (B); 6.6–8.0, 70 to 75% (B); 8.0–8.5 min, 75 to 100% (B); 8.50–9.5 min, 100% (B); 9.5–9.6 min, 100% to 5% (B); 9.6–12.0 min, 5% (B). Detection and quantification were performed by scheduled- Multiple Reaction Monitoring (MRM) using 1 ms pause time and 50 ms dwell times to achieve sufficient points per peak. The interface parameters and common settings were as follows: interface voltage: 1 kV; nebulizing gas flow: 3 L/min; heating gas flow: 10 L/min; drying gas flow: 10 L/min; interface temperature: 400 °C; desolvation line (DL) temperature: 150 °C; heat block temperature: 500 °C; collision gas pressure 300 kPa. Compound-specific MRM parameters are shown in **Supplementary File 1c**.

Enzyme-linked immunosorbent assay (ELISA)

Steroids were extracted from testicular homogenates and from organotypic culture media with 5 volumes of diethyl ether (Carlo Erba). The organic phase was then recovered and evaporated in a water bath at 37°C. The tubes were stored at -20°C until use.

Progesterone and estradiol levels were measured in 50 µL of testicular homogenates and in 50 µL of culture media using Cayman ELISA kit (582601 for progesterone and 501890 for estradiol, Cayman Chemical Company, Ann Arbor, MI, USA), according to the supplier's recommendations. The sensitivity limit for the progesterone assay was 10 pg/mL with average intra- and inter-trial variations of 13.9% and 9.6%, respectively. The sensitivity limit for the estradiol assay was 20 pg/mL and the lower limit of detection was 6 pg/mL with average intra- and inter-trial variations of 20.25% and 14.975%, respectively.

Aromatase activity

After homogenization of ~10-50 mg of tissues in 500 μL of Aromatase Assay Buffer, the aromatase activity was measured with the fluorometric Aromatase (CYP19A) Activity assay kit (ab273306; Abcam) according to the manufacturer's instructions.

Radioimmunoassay (RIA)

INSL3 was assayed by using RIA kit with ^{125}I as tracer (RK-035-27, Phoenix Pharmaceuticals, Strasbourg, France). According to the manufacturer's instructions, analyses were performed on 100 μL of culture media or tissue homogenates. Assay validation was assessed by determining the recovery of expected amounts of INSL3 in samples to which exogenous INSL3 was added. The sensitivity of the INSL3 RIA kit was 60.4 pg/mL and the range of the assay was 10-1280 pg/mL.

Statistical analyses

Statistical analyses were carried out with GraphPad Prism 8 software (GraphPad Software Inc., La Jolla, CA, USA). Data are presented as means ± SEM. The non-parametric Mann-Whitney test was used to compare *in vitro* cultures and *in vivo* controls (D16 FT *vs* 22 d*pp*, D16 CSF *vs* 22 d*pp*, D30 FT *vs* 36 d*pp*, D30 CSF *vs* 36 d*pp*, D30 FT + hCG *vs* 36 d*pp*, D30 CSF + hCG *vs* 36 d*pp*); cultures of fresh and CSF tissues (6 d*pp* *vs* 6 d*pp* CSF, D16 FT *vs* D16 CSF, D30 FT *vs* D30 CSF, D30 FT + hCG *vs* D30 CSF + hCG); cultures with or without hCG (D30 FT + hCG *vs* D30 FT, D30 CSF + hCG *vs* D30 CSF). A value of $P < 0.05$ was considered statistically significant.

Conflict of Interest

The authors declare that the research was conducted in the absence of any commercial or financial relationships that could be construed as a potential conflict of interest.

Funding

This work was supported by a PhD grant from Région Normandie (awarded to LM) and by fundings from Ligue contre le Cancer Comité de Seine-Maritime (awarded to CR), France Lymphome Espoir (Bourse Sacha awarded to CR), Région Normandie and Europe (RIN Steroids awarded to HL) and ANR (ANR-21-CE14-0068, sc-SpermInVitro awarded to NR). The funders had no role in study design, data collection and analysis, decision to publish, or preparation of the manuscript.

Acknowledgements

Data from RT-qPCR and images were obtained on PRIMACEN (http://www.primacen.fr), the Cell Imaging Platform of Normandy, IRIB, Faculty of Sciences, University of Rouen, 76821 Mont-Saint-Aignan. The authors also thank the U1096 team for the access to their western blot devices.

References

1. Allen CM, Lopes F, Mitchell RT, Spears N. How does chemotherapy treatment damage the prepubertal testis? Reproduction. 2018 Dec;R209–33.

2. Miller KD, Siegel RL, Lin CC, Mariotto AB, Kramer JL, Rowland JH, et al. Cancer treatment and survivorship statistics, 2016. CA: A Cancer Journal for Clinicians. 2016 Jul;66(4):271–89.

3. Sato T, Katagiri K, Gohbara A, Inoue K, Ogonuki N, Ogura A, et al. In vitro production of functional sperm in cultured neonatal mouse testes. Nature. 2011 Mar 24;471(7339):504–7.

4. Yokonishi T, Sato T, Komeya M, Katagiri K, Kubota Y, Nakabayashi K, et al. Offspring production with sperm grown in vitro from cryopreserved testis tissues. Nat Commun. 2014 Sep;5(1):4320.

5. Arkoun B, Dumont L, Milazzo JP, Way A, Bironneau A, Wils J, et al. Retinol Improves In Vitro Differentiation of Pre-Pubertal Mouse Spermatogonial Stem Cells into Sperm during the First Wave of Spermatogenesis. Schlatt S, editor. PLoS ONE. 2015 Feb 25;10(2):e0116660.

6. Dumont L, Arkoun B, Jumeau F, Milazzo JP, Bironneau A, Liot D, et al. Assessment of the optimal vitrification protocol for pre-pubertal mice testes leading to successful in vitro production of flagellated spermatozoa. Andrology. 2015 May;3(3):611–25.

7. Dumont L, Oblette A, Rondanino C, Jumeau F, Bironneau A, Liot D, et al. Vitamin A prevents round spermatid nuclear damage and promotes the production of motile sperm during *in vitro* maturation of vitrified pre-pubertal mouse testicular tissue. Mol Hum Reprod. 2016 Sep 25;molehr;gaw063v2.

8. Rondanino C, Maouche A, Dumont L, Oblette A, Rives N. Establishment, maintenance and functional integrity of the blood–testis barrier in organotypic cultures of fresh and frozen/thawed prepubertal mouse testes. MHR: Basic science of reproductive medicine. 2017 May;23(5):304–20.

9. Pence LM, Schmitt TC, Beger RD, Del Valle PL, Nakamura N. Testicular function in cultured postnatal mouse testis fragments is similar to that of animals during the first wave of spermatogenesis. Birth Defects Research. 2019 Mar 15;111(5):270–80.

10. Dumont L, Lopez Maestre H, Chalmel F, Huber L, Rives-Feraille A, Moutard L, et al. Throughout in vitro first spermatogenic wave: Next-generation sequencing gene expression patterns of fresh and cryopreserved prepubertal mice testicular tissue explants. Front Endocrinol (Lausanne). 2023;14:1112834.

11. O'Shaughnessy PJ, Willerton L, Baker PJ. Changes in Leydig cell gene expression during development in the mouse. Biol Reprod. 2002 Apr;66(4):966–75.

12. Sararols P, Stévant I, Neirijnck Y, Rebourcet D, Darbey A, Curley MK, et al. Specific Transcriptomic Signatures and Dual Regulation of Steroidogenesis Between Fetal and Adult Mouse Leydig Cells. Front Cell Dev Biol. 2021 Jun 28;9:695546.

13. O'Shaughnessy PJ, Baker PJ, Heikkilä M, Vainio S, McMahon AP. Localization of 17beta-hydroxysteroid dehydrogenase/17-ketosteroid reductase isoform expression in the developing mouse testis--androstenedione is the major androgen secreted by fetal/neonatal leydig cells. Endocrinology. 2000 Jul;141(7):2631–7.

726 14. Ye L, Li X, Li L, Chen H, Ge RS. Insights into the Development of the Adult Leydig Cell Lineage
727 from Stem Leydig Cells. Front Physiol. 2017 Jun 28;8:430.

728 15. Jiang MH, Cai B, Tuo Y, Wang J, Zang ZJ, Tu X, et al. Characterization of Nestin-positive stem
729 Leydig cells as a potential source for the treatment of testicular Leydig cell dysfunction. Cell
730 Res. 2014 Dec;24(12):1466–85.

731 16. Zhang F ping, Pakarainen T, Zhu F, Poutanen M, Huhtaniemi I. Molecular Characterization of
732 Postnatal Development of Testicular Steroidogenesis in Luteinizing Hormone Receptor
733 Knockout Mice. Endocrinology. 2004 Mar;145(3):1453–63.

734 17. Ge RS, Hardy MP. Variation in the End Products of Androgen Biosynthesis and Metabolism
735 during Postnatal Differentiation of Rat Leydig Cells*. Endocrinology. 1998 Sep 1;139(9):3787–
736 95.

737 18. Balvers M, Spiess AN, Domagalski R, Hunt N, Kilic E, Mukhopadhyay AK, et al. Relaxin-like factor
738 expression as a marker of differentiation in the mouse testis and ovary. Endocrinology. 1998
739 Jun;139(6):2960–70.

740 19. Mendis-Handagama SMLC, Ariyaratne HBS, Mrkonjich L, Ivell R. Expression of insulin-like
741 peptide 3 in the postnatal rat Leydig cell lineage: timing and effects of triiodothyronine-
742 treatment. Reproduction. 2007 Feb;133(2):479–85.

743 20. Wu L, Einstein M, Geissler WM, Chan HK, Elliston KO, Andersson S. Expression cloning and
744 characterization of human 17 beta-hydroxysteroid dehydrogenase type 2, a microsomal
745 enzyme possessing 20 alpha-hydroxysteroid dehydrogenase activity. J Biol Chem. 1993 Jun
746 15;268(17):12964–9.

747 21. Li X, Wang Z, Jiang Z, Guo J, Zhang Y, Li C, et al. Regulation of seminiferous tubule-associated
748 stem Leydig cells in adult rat testes. Proc Natl Acad Sci USA. 2016 Mar 8;113(10):2666–71.

749 22. Hu GX, Lin H, Chen GR, Chen BB, Lian QQ, Hardy DO, et al. Deletion of the Igf1 gene:
750 suppressive effects on adult Leydig cell development. J Androl. 2010 Aug;31(4):379–87.

751 23. Wang GM, O'Shaughnessy PJ, Chubb C, Robaire B, Hardy MP. Effects of insulin-like growth
752 factor I on steroidogenic enzyme expression levels in mouse leydig cells. Endocrinology. 2003
753 Nov;144(11):5058–64.

754 24. Ma X, Dong Y, Matzuk MM, Kumar TR. Targeted disruption of luteinizing hormone beta-subunit
755 leads to hypogonadism, defects in gonadal steroidogenesis, and infertility. Proc Natl Acad Sci U
756 S A. 2004 Dec 7;101(49):17294–9.

757 25. De Gendt K, Swinnen JV, Saunders PTK, Schoonjans L, Dewerchin M, Devos A, et al. A Sertoli
758 cell-selective knockout of the androgen receptor causes spermatogenic arrest in meiosis. Proc
759 Natl Acad Sci U S A. 2004 Feb 3;101(5):1327–32.

760 26. Chang C, Chen YT, Yeh SD, Xu Q, Wang RS, Guillou F, et al. Infertility with defective
761 spermatogenesis and hypotestosteronemia in male mice lacking the androgen receptor in
762 Sertoli cells. Proc Natl Acad Sci U S A. 2004 May 4;101(18):6876–81.

763 27. Holdcraft RW, Braun RE. Androgen receptor function is required in Sertoli cells for the terminal
764 differentiation of haploid spermatids. Development. 2004 Jan 15;131(2):459–67.

765 28. O'Shaughnessy PJ, Monteiro A, Abel M. Testicular development in mice lacking receptors for
766 follicle stimulating hormone and androgen. PLoS One. 2012;7(4):e35136.

767 29. Hagenäs L, Ritzén EM, Ploöen L, Hansson V, French FS, Nayfeh SN. Sertoli cell origin of testicular
768 androgen-binding protein (ABP). Mol Cell Endocrinol. 1975 May;2(5):339–50.

769 30. Robertson KM, O'Donnell L, Jones ME, Meachem SJ, Boon WC, Fisher CR, et al. Impairment of
770 spermatogenesis in mice lacking a functional aromatase (cyp 19) gene. Proc Natl Acad Sci U S A.
771 1999 Jul 6;96(14):7986–91.

772 31. Sinkevicius KW, Laine M, Lotan TL, Woloszyn K, Richburg JH, Greene GL. Estrogen-dependent
773 and -independent estrogen receptor-alpha signaling separately regulate male fertility.
774 Endocrinology. 2009 Jun;150(6):2898–905.

775 32. Rommerts FF, de Jong FH, Brinkmann AO, van der Molen HJ. Development and cellular
776 localization of rat testicular aromatase activity. J Reprod Fertil. 1982 Jul;65(2):281–8.

777 33. Papadopoulos V, Carreau S, Szerman-Joly E, Drosdowsky MA, Dehennin L, Scholler R. Rat testis
778 17 beta-estradiol: identification by gas chromatography-mass spectrometry and age related
779 cellular distribution. J Steroid Biochem. 1986 Jun;24(6):1211–6.

780 34. Nitta H, Bunick D, Hess RA, Janulis L, Newton SC, Millette CF, et al. Germ cells of the mouse
781 testis express P450 aromatase. Endocrinology. 1993 Mar;132(3):1396–401.

782 35. Maclean JA, Chen MA, Wayne CM, Bruce SR, Rao M, Meistrich ML, et al. Rhox: a new
783 homeobox gene cluster. Cell. 2005 Feb 11;120(3):369–82.

784 36. Willems A, De Gendt K, Allemeersch J, Smith LB, Welsh M, Swinnen JV, et al. Early effects of
785 Sertoli cell-selective androgen receptor ablation on testicular gene expression. Int J Androl.
786 2010 Jun 1;33(3):507–17.

787 37. Zhou Q, Nie R, Prins GS, Saunders PTK, Katzenellenbogen BS, Hess RA. Localization of Androgen
788 and Estrogen Receptors in Adult Male Mouse Reproductive Tract. Journal of Andrology.
789 2002;12.

790 38. Kotula-Balak M, Pawlicki P, Milon A, Tworzydlo W, Sekula M, Pacwa A, et al. The role of G-
791 protein-coupled membrane estrogen receptor in mouse Leydig cell function—in vivo and in
792 vitro evaluation. Cell Tissue Res. 2018 Nov;374(2):389–412.

793 39. Lucas TFG, Royer C, Siu ER, Lazari MFM, Porto CS. Expression and signaling of G protein-coupled
794 estrogen receptor 1 (GPER) in rat sertoli cells. Biol Reprod. 2010 Aug 1;83(2):307–17.

795 40. Chimento A, Sirianni R, Delalande C, Silandre D, Bois C, Andò S, et al. 17β-Estradiol activates
796 rapid signaling pathways involved in rat pachytene spermatocytes apoptosis through GPR30
797 and ERα. Molecular and Cellular Endocrinology. 2010 May;320(1–2):136–44.

798 41. Chimento A, Sirianni R, Zolea F, Bois C, Delalande C, Andò S, et al. Gper and ESRs are expressed
799 in rat round spermatids and mediate oestrogen-dependent rapid pathways modulating
800 expression of cyclin B1 and Bax: Gper and ESR involvement in rat round spermatid maturation.
801 International Journal of Andrology. 2011 Oct;34(5pt1):420–9.

802 42. Grimaldi P, Pucci M, Di Siena S, Di Giacomo D, Pirazzi V, Geremia R, et al. The faah gene is the
803 first direct target of estrogen in the testis: role of histone demethylase LSD1. Cell Mol Life Sci.
804 2012 Dec;69(24):4177–90.

805 43. Rossi G, Gasperi V, Paro R, Barsacchi D, Cecconi S, Maccarrone M. Follicle-stimulating hormone
806 activates fatty acid amide hydrolase by protein kinase A and aromatase-dependent pathways in
807 mouse primary Sertoli cells. Endocrinology. 2007 Mar;148(3):1431–9.

808 44. Kuo PL, Tseng JY, Chen HI, Wu CY, Omar HA, Wang CY, et al. Identification of SEPTIN12 as a
809 novel target of the androgen and estrogen receptors in human testicular cells. Biochimie. 2019
810 Mar;158:1–9.

811 45. Milazzo JP, Vaudreuil L, Cauliez B, Gruel E, Masse L, Mousset-Simeon N, et al. Comparison of
812 conditions for cryopreservation of testicular tissue from immature mice. Human Reproduction.
813 2008 Jan;23(1):17–28.

814 46. Berthois Y, Katzenellenbogen JA, Katzenellenbogen BS. Phenol red in tissue culture media is a
815 weak estrogen: implications concerning the study of estrogen-responsive cells in culture. Proc
816 Natl Acad Sci USA. 1986 Apr;83(8):2496–500.

817 47. Bustin SA, Benes V, Garson JA, Hellemans J, Huggett J, Kubista M, et al. The MIQE Guidelines:
818 Minimum Information for Publication of Quantitative Real-Time PCR Experiments. Clinical
819 Chemistry. 2009 Apr 1;55(4):611–22.

820 48. Gong ZK, Wang SJ, Huang YQ, Zhao RQ, Zhu QF, Lin WZ. Identification and validation of suitable
821 reference genes for RT-qPCR analysis in mouse testis development. Mol Genet Genomics. 2014
822 Dec;289(6):1157–69.

823 49. Cacciola G, Chioccarelli T, Altucci L, Ledent C, Mason JI, Fasano S, et al. Low 17beta-Estradiol
824 Levels in Cnr1 Knock-Out Mice Affect Spermatid Chromatin Remodeling by Interfering with
825 Chromatin Reorganization. Biology of Reproduction. 2013 Jun 20;88(6):152–152.

826 50. Livak KJ, Schmittgen TD. Analysis of Relative Gene Expression Data Using Real-Time
827 Quantitative PCR and the 2−ΔΔCT Method. Methods. 2001 Dec;25(4):402–8.

828 51. O'Shaughnessy PJ, Mitchell RT, Monteiro A, O'Hara L, Cruickshanks L, der Grinten HC van, et al.
829 Androgen receptor expression is required to ensure development of adult Leydig cells and to
830 prevent development of steroidogenic cells with adrenal characteristics in the mouse testis.
831 BMC Dev Biol. 2019 Dec;19(1):8.

832 52. Radovic Pletikosic SM, Starovlah IM, Miljkovic D, Bajic DM, Capo I, Nef S, et al. Deficiency in
833 insulin-like growth factors signalling in mouse Leydig cells increase conversion of testosterone
834 to estradiol because of feminization. Acta Physiol [Internet]. 2021 Mar [cited 2022 Feb
835 25];231(3). Available from: https://onlinelibrary.wiley.com/doi/10.1111/apha.13563

836 53. Yao J, Zuo H, Gao J, Wang M, Wang D, Li X. The effects of IGF-1 on mouse spermatogenesis
837 using an organ culture method. Biochemical and Biophysical Research Communications. 2017
838 Sep;491(3):840–7.

839 54. Cannarella R, Condorelli RA, Mongioì LM, Barbagallo F, Calogero AE, La Vignera S. Effects of the
840 selective estrogen receptor modulators for the treatment of male infertility: a systematic
841 review and meta-analysis. Expert Opinion on Pharmacotherapy. 2019 Aug 13;20(12):1517–25.

842 55. Kooshesh L, Bahmanpour S, Zeighami S, Nasr-Esfahani MH. Effect of Letrozole on sperm
843 parameters, chromatin status and ROS level in idiopathic Oligo/Astheno/Teratozoospermia.
844 Reprod Biol Endocrinol. 2020 Dec;18(1):47.

845 56. Shuling L, Sie Kuei ML, Saffari SE, Jiayun Z, Yeun TT, Leng JPW, et al. Do men with normal
846 testosterone–oestradiol ratios benefit from letrozole for the treatment of male infertility?
847 Reproductive BioMedicine Online. 2019 Jan;38(1):39–45.

848 57. Lue Y, Wang C, Lydon JP, Leung A, Li J, Swerdloff RS. Functional role of progestin and the
849 progesterone receptor in the suppression of spermatogenesis in rodents. Andrology. 2013
850 Mar;1(2):308–17.

851 58. O'Hara L, McInnes K, Simitsidellis I, Morgan S, Atanassova N, Slowikowska-Hilczer J, et al.
852 Autocrine androgen action is essential for Leydig cell maturation and function, and protects
853 against late-onset Leydig cell apoptosis in both mice and men. FASEB j. 2015 Mar;29(3):894–
854 910.

855 59. El Kharraz S, Dubois V, Royen ME, Houtsmuller AB, Pavlova E, Atanassova N, et al. The androgen
856 receptor depends on ligand-binding domain dimerization for transcriptional activation. EMBO
857 Rep [Internet]. 2021 Dec 6 [cited 2021 Dec 14];22(12). Available from:
858 https://onlinelibrary.wiley.com/doi/10.15252/embr.202152764

859 60. Schauwaers K, De Gendt K, Saunders PTK, Atanassova N, Haelens A, Callewaert L, et al. Loss of
860 androgen receptor binding to selective androgen response elements causes a reproductive
861 phenotype in a knockin mouse model. Proc Natl Acad Sci USA. 2007 Mar 20;104(12):4961–6.

862 61. Zanatta AP, Gonçalves R, Ourique da Silva F, Pedrosa RC, Zanatta L, Bouraïma-Lelong H, et al.
863 Estradiol and 1α,25(OH)2 vitamin D3 share plasma membrane downstream signal transduction
864 through calcium influx and genomic activation in immature rat testis. Theriogenology. 2021
865 Sep;172:36–46.

866 62. Genissel C, Levallet J, Carreau S. Regulation of cytochrome P450 aromatase gene expression in
867 adult rat Leydig cells: comparison with estradiol production. Journal of Endocrinology. 2001 Jan
868 1;168(1):95–105.

869 63. Laguë É, Tremblay JJ. Estradiol represses Insulin-like 3 expression and promoter activity in MA-
870 10 Leydig cells. Toxicology. 2009 Apr 28;258(2–3):101–5.

871 64. Song WC. The Role of Estrogen Sulfotransferase in Leydig Cells. In: Payne AH, Hardy MP,
872 editors. The Leydig Cell in Health and Disease [Internet]. Totowa, NJ: Humana Press; 2007 [cited
873 2022 Feb 3]. p. 197–205. (Contemporary Endocrinology). Available from:
874 http://link.springer.com/10.1007/978-1-59745-453-7_14

875 65. Qian YM, Sun XJ, Tong MH, Li XP, Richa J. Targeted Disruption of the Mouse Estrogen
876 Sulfotransferase Gene Reveals a Role of Estrogen Metabolism in Intracrine and Paracrine
877 Estrogen Regulation. 2001;9.

878 66. Tong MH, Christenson LK, Song WC. Aberrant Cholesterol Transport and Impaired
879 Steroidogenesis in Leydig Cells Lacking Estrogen Sulfotransferase. Endocrinology. 2004 May
880 1;145(5):2487–97.

881 67. Wu X, Arumugam R, Zhang N, Lee MM. Androgen profiles during pubertal Leydig cell
882 development in mice. REPRODUCTION. 2010 Jul;140(1):113–21.

Figure captions

Figure 1. Leydig cells are partially mature after 30 days of organotypic culture. (A) Representative images of 3β-HSD expression by Leydig cells during mouse postnatal development (6 d*pp*, 22 d*pp* and 36 d*pp*) and in *in vitro* cultured tissues after 16 days of culture (D16) or 30 days (D30). A representative image of a negative control, carried out by omitting the primary antibody, is also shown. Testicular tissue sections were counterstained with Hoechst (blue). Dotted lines delineate seminiferous tubules. Scale: 15 µm. (B) Number of 3β-HSD+ Leydig cells per cm² of testicular tissue during mouse postnatal development (6 d*pp*, 22 d*pp* and 36 d*pp*) and in *in vitro* cultured tissues (D16 and D30). (C-D) Percentage of Leydig cells (C) in apoptosis (3β-HSD and cleaved caspase 3 positive) or (D) in proliferation (3β-HSD and Ki67 positive) in *in vivo* and *in vitro* matured tissues. (E) Percentage of 3β-HSD positive Leydig cells expressing AR in *in vivo* and *in vitro* matured tissues. (F-J) Relative mRNA levels of Leydig cell differentiation factors (*Igf1*, *Dhh*), progenitor/immature Leydig cell (*Srd5a1*) and adult Leydig cell markers (*Sult1e1*, *Insl3*) (normalized to *Gapdh* and *Actb* or to *Hsd3b1*). (K) Intratesticular concentration of INSL3 (pg/mg of tissue) or in the culture medium (pg/mL).

Data are presented as means ± SEM with n = 4 biological replicates for each group. A value of $*P < 0.05$ was considered statistically significant. n.d.: not determined (under the detection limit)

FT: Fresh Tissue; CSF: Controlled Slow Freezing.

Figure 1 – figure supplement 1. Impact of controlled slow freezing on Leydig cells in organotypic cultures. (A) Representative images of 3β-HSD expression in Leydig cells at 6 d*pp* and in *in vitro* cultured fresh (FT) or frozen/thawed (CSF) testicular tissues (D16 and D30). Testicular tissue sections were counterstained with Hoechst (blue). Dotted lines delineate seminiferous tubules. Scale: 15 µm. (B) Number of 3β-HSD positive Leydig cells per cm² of FT or CSF testicular tissue. (C-D) Percentage of Leydig cells (C) in apoptosis (3β-HSD and cleaved caspase 3 positive) or (D) in proliferation (3β-HSD and Ki67 positive) in *in vivo* and *in vitro* matured FT or CSF tissues. (E) Percentage of 3β-HSD positive Leydig cells expressing AR in *in vivo* and *in vitro* matured FT or CSF tissues. (F-J) Relative mRNA levels of Leydig cell differentiation factors (*Igf1*, *Dhh*), progenitor/immature Leydig cell (*Srd5a1*)

and of adult Leydig cell markers (*Sult1e1*, *Insl3*) (normalized to *Gapdh* and *Actb* or to *Hsd3b1*).

Data are presented as means ± SEM with n = 4 biological replicates for each group. A value of $*P < 0.05$ was considered statistically significant.

FT: Fresh Tissue, CSF: Controlled Slow Freezing

Figure 2. The expression of several actors of steroidogenesis is downregulated in 30-day organotypic cultures. (A-I) Relative mRNA levels of *Lhcgr*, *Star*, *Cyp11a1*, *Hsd3b1*, *Cyp17a1*, *Hsd17b3* and *Hsd17b2* (normalized to *Gapdh* and *Actb* or to *Hsd3b1*) and relative protein levels of 3β-HSD (normalized to ACTB) and CYP17A1 (normalized to 3β-HSD) during mouse postnatal development (6 d*pp*, 22 d*pp* and 36 d*pp*) and in *in vitro* cultured FT or CSF tissues (D16 and D30). (J) Representative images of CYP17A1 expression during mouse postnatal development (22 d*pp* and 36 d*pp*) and in *in vitro* cultured tissues (D16 and D30). A representative image of a negative control, carried out by omitting the primary antibody, is also shown. Testicular tissue sections were counterstained with Hoechst (blue). Dotted lines delineate seminiferous tubules. Scale: 15 µm.

Data are presented as means ± SEM with n = 4 biological replicates for each group. A value of $*P < 0.05$ was considered statistically significant.

Figure. 3: An increased production of progesterone and estradiol and a decreased production of androstenedione are observed after 16 and 30 days of culture of prepubertal mouse testicular tissues. Intratesticular concentrations of (A) progesterone, (B) androstenedione, (C) testosterone and (D) estradiol during mouse postnatal development (6 d*pp*, 22 d*pp* and 36 d*pp*) and in *in vitro* cultured fresh (FT) or frozen/thawed (CSF) tissues (D16 and D30). Steroid concentrations were normalized to protein levels. (E-F) Concentrations of (E) progesterone, androstenedione, testosterone and (F) estradiol in the culture medium of FT tissues. (G) Intratesticular concentrations of total, free and esterified cholesterol normalized to tissue mass.

Data are presented as means ± SEM with n = 4 biological replicates for each group. A value of $*P < 0.05$ was considered statistically significant.

Figure 3 – figure supplement 1. **Impact of controlled slow freezing on steroids production by Leydig cells in organotypic cultures.** Concentrations of androgens

(androstenedione and testosterone) in the culture medium of fresh (FT) or frozen/thawed (CSF) testicular tissues.

Data are presented as means ± SEM with n = 4 biological replicates for each group. A value of $*P < 0.05$ was considered statistically significant.

Figure. 4: Androgen signaling is altered in 30-day organotypic cultures. (A) Relative mRNA levels of *Ar* (normalized to *Gapdh* and *Actb*) and (B) relative protein levels of AR (normalized to ACTB) during mouse postnatal development (6 d*pp*, 22 d*pp* and 36 d*pp*) and in *in vitro* cultured FT or CSF tissues (D16 and D30). (C) Representative images of AR expression at 22 d*pp* and 36 d*pp* and at corresponding *in vitro* time points (D16 and D30). A representative image of a negative control is shown in Figure 2J (same secondary antibody as for CYP17A1). Testicular tissue sections were counterstained with Hoechst (blue). Solid arrowheads: peritubular myoid cells. Open arrowheads: Sertoli cells. Arrows: Leydig cells. Dotted lines delineate seminiferous tubules (ST). Scale: 15 µm. (D-G) Relative mRNA levels of *Rhox5*, *Septin12*, *Eppin* and *Abp* (normalized to *Gapdh* and *Actb*).

Data are presented as means ± SEM with n = 4 biological replicates for each group. A value of $*P < 0.05$ was considered statistically significant.

Figure. 5: The expression of aromatase and estrogen signaling are impaired after 30 days of organotypic culture. (A) Relative mRNA levels of *Cyp19a1* (normalized to *Gapdh* and *Actb*) and (B) relative protein levels of CYP19A1 (normalized to ACTB) during mouse postnatal development (6 d*pp*, 22 d*pp* and 36 d*pp*) and in *in vitro* cultured FT or CSF tissues (D16 and D30). The bands on the western blot correspond to different isoforms of CYP19. (C) Representative images of CYP19A1 expression at 6 d*pp*, 22 d*pp* and 36 d*pp* and at corresponding *in vitro* time points (D16 and D30). A representative image of a negative control, carried out by omitting the primary antibody, is also shown. Testicular tissue sections were counterstained with Hematoxylin. Scale: 15 µm. Arrow: Leydig cells. Arrowheads: elongated spermatids. (D) Aromatase activity (normalized to tissue weight). (E-G) Relative mRNA levels of *Esr1*, *Esr2* and *Gper1* (normalized to *Gapdh* and *Actb*). (H) Relative mRNA levels of *Faah* (normalized to *Gapdh* and *Actb*) and (I) relative protein levels of FAAH (normalized to ACTB). The second band at 80 kDa is an isoform of FAAH (Q8BRM1, UniProtKB).

Data are presented as means ± SEM with n = 4 biological replicates for each group. A value of $*P < 0.05$ was considered statistically significant.

Figure. 6: hCG is insufficient to stimulate Leydig cell differentiation and restore steroidogenesis and steroid hormone signaling. (A-D) Levels of androgens (androstenedione and testosterone) (A-B) in testicular tissues and (C-D) in culture medium with 1 nM hCG or without supplementation. (E-S) Relative mRNA levels of genes involved in steroidogenesis and androgen/estrogen signaling pathways (normalized to *Gapdh* and *Actb* or to *Hsd3b1*) with or without hCG supplementation. (T) Proportion of seminiferous tubules containing the most advanced type of germ cells after *in vitro* culture with or without hCG. $P < 0.05$: * *vs* 36 d*pp* and # *vs* D30 FT. (U) Sertoli cell number in seminiferous tubules after *in vitro* culture with or without hCG.

Data are presented as means ± SEM with n = 4 biological replicates for each group. A value of $*P < 0.05$ was considered statistically significant. FT: Fresh Tissue; CSF: Controlled Slow Freezing.

Figure 6 – figure supplement 1. **Impact of different hCG concentrations on testosterone production in organotypic cultures.** (A) Concentrations of testosterone in the culture medium after supplementation with different hCG concentrations (5 pM, 50 pM, 1 nM, 5 nM, 50 nM) from D16 to D30. (B) Concentrations of testosterone in FT testicular tissues (D30) normalized to *in vivo* control (36 d*pp*) and in culture medium at D30 normalized to *in vitro* control without hCG, after supplementation with different hCG concentrations (5 pM, 50 pM, 1 nM, 5 nM, 50 nM).

Data are presented as means ± SEM with n = 4 biological replicates for each group. A value of $*P < 0.05$ was considered statistically significant.

Figure 6 – figure supplement 2. **Impact of hCG supplementation on mRNA levels of genes involved in steroidogenesis and androgen signaling in organotypic cultures.** Relative mRNA levels of Leydig cell markers, actors of steroidogenesis and androgen signaling (normalized to *Gapdh* and *Actb* or to *Hsd3b1*) after supplementation with 1 nM hCG.

Data are presented as means ± SEM with n = 4 biological replicates for each group. A value of $*P < 0.05$ was considered statistically significant.

Figure. 7: Altered steroidogenesis and androgen/estrogen signaling pathways in *in vitro* matured testicular tissues of prepubertal mice A similar density of Leydig cells is found

after 30 days of organotypic culture (D30) and at 36 days *postpartum*, the corresponding *in vivo* time point. However, Leydig cells are partially mature *in vitro* with a decrease in *Sult1e1* and *Insl3* mRNA levels (adult Leydig cell markers). The mRNA levels of *Cyp11a1*, *Cyp17a1* and *Hsd17b3* encoding steroidogenic enzymes and the protein levels of CYP17A1 are decreased *in vitro*. Increased amounts of cholesterol, progesterone and estradiol and decreased androstenedione intratesticular levels are observed at D30. Furthermore, despite testosterone levels similar to *in vivo*, the expression of the androgen receptor (AR) and of the androgen binding protein (*Abp*), androgen signaling is altered at D30, with decreased transcript levels of the androgen target gene *Rhox5* and of *Septin12*. Moreover, with decreased expression and activity of aromatase and decreased estrogen receptor expression, estrogen signaling is impaired at D30, leading to decreased transcript and protein levels of the estrogen target gene *Faah*.

Figure 8. Scheme of the study design. At 6 d*pp* (D0), the testis contains only spermatogonia and the initiation of meiosis occurs between 7 and 9 d*pp*. At 22 d*pp* (D16), meiosis ends and the first round spermatids appear. At 36 d*pp* (D30), the first spermatozoa appear and this is the end of the first spermatogenic wave. Arrows represent times at which the medium was collected (D0, D2, D6, D10, D14, D18, D22, D26 and D30).
BM: Basal Medium; CSF: Controlled Slow Freezing; d*pp*: days *postpartum*; hCG: human Chorionic Gonadotropin; KSR: KnockOut Serum replacement; PR-: without phenol red; Rol: retinol

Figure 8 – figure supplement 1. (A) Testicular tissue area (in mm^2) measured on tissue sections from mice of different ages (6 d*pp*, 22 d*pp* and 36 d*pp*) and after 16 days (D16) or 30 days (D30) of organotypic cultures. (B) Necrotic region (percentage of the tissue section area) at D16 and D30. (C-D) Representative images of cleaved caspase 3 (CC3) immunostaining, mostly detected in the central necrotic region (dotted lines). Testicular tissue sections were counterstained with Hoechst (blue). Scale: 100 µm. (E-F) Representative images of PAS staining, with the necrotic area delineated by dotted lines. Testicular tissue sections were counterstained with hematoxylin. Scale: 200 µm.
Data are presented as means ± SEM with n = 4 biological replicates for each group. A value of $*P < 0.05$ was considered statistically significant.
FT: Fresh Tissue; CSF: Controlled Slow Freezing.

Supporting information

Supplementary File 1a. Detailed list of antibodies used in this study HRP: horseradish peroxidase; IF: immunofluorescence; IHC: immunohistochemistry; O/N: overnight; RT: room temperature; WB: western blot

Supplementary File 1b. List of PCR primers used in this study

Supplementary File 1c. Compound-specific MRM parameters for LC-MS/MS CE: collision energy; DHEA: Dehydroepiandrosterone; MRM: multiple reaction monitoring

Supplementary File 2. Western Blot for 3β-HSD, CYP17A1, AR, CYP19 and FAAH.

Figure 1-source data 1: Source data of figure 1

Figure 1-figure supplement 1-source data 1: Source data of figure 1 – figure supplement 1

Figure 2-source data 1: Source data of figure 2

Figure 3-source data 1: Source data of figure 3

Figure 3-figure supplement 1-source data 1: Source data of figure 3 – figure supplement 1

Figure 4-source data 1: Source data of figure 4

Figure 5-source data 1: Source data of figure 5

Figure 6-source data 1: Source data of figure 6

Figure 6-figure supplement 1-source data 1: Source data of figure 6 – figure supplement 1

Figure 6-figure supplement 1-source data 2: Source data of figure 6 – figure supplement 2

Figure 8-figure supplement 1-source data 1: Source data of figure 8 – figure supplement 1

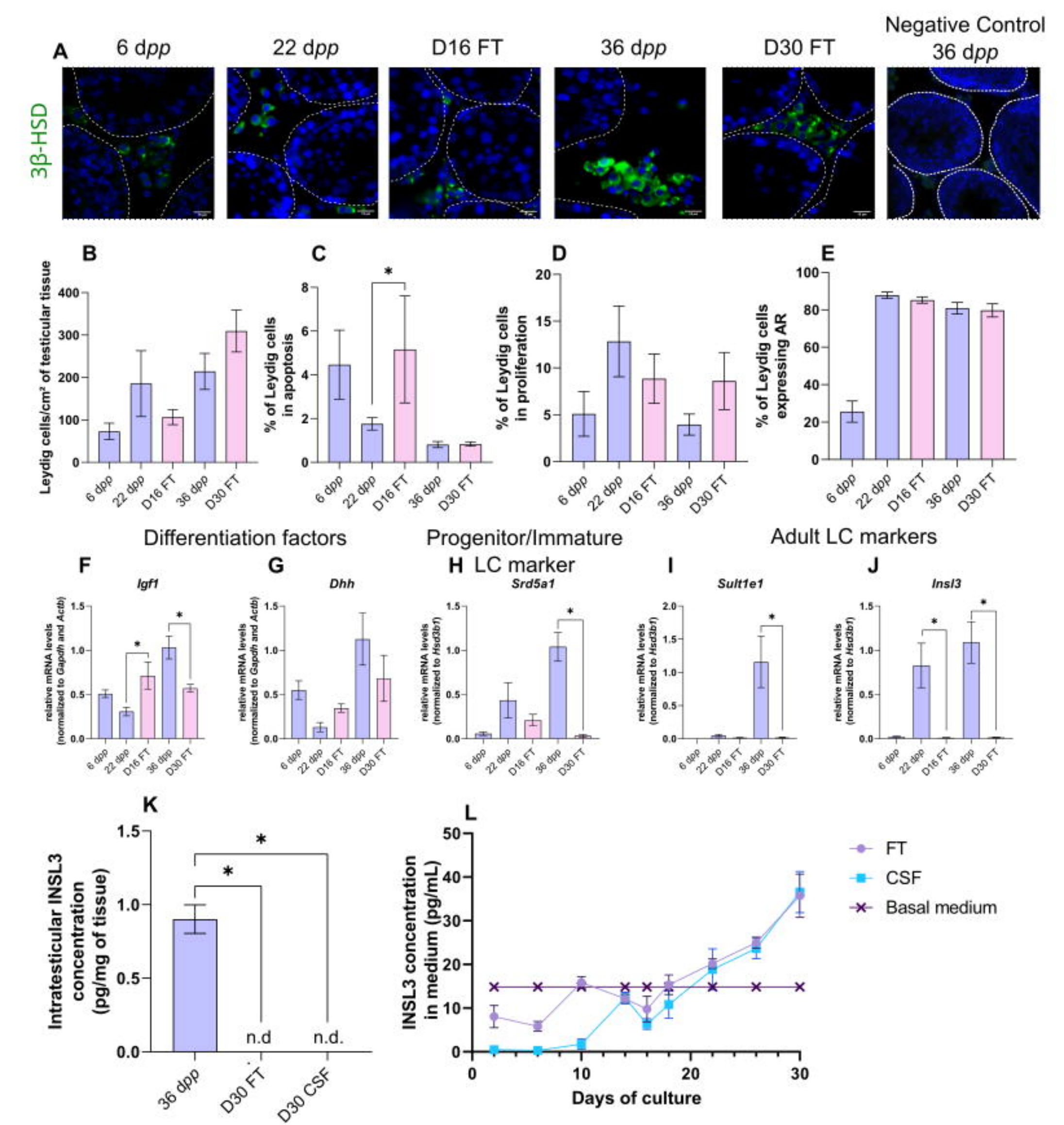
A
6 dpp
22 dpp
D16 FT
36 dpp
D30 FT
Negative Control 36 dpp
3β-HSD
B
Leydig cells/cm² of testicular tissue
C
% of Leydig cells in apoptosis
D
% of Leydig cells in proliferation
E
% of Leydig cells expressing AR
6 dpp
22 dpp
D16 FT
36 dpp
D30 FT
Differentiation factors
Progenitor/Immature
Adult LC markers
F
Igf1
G
Dhh
H LC marker
Srd5a1
I
Sult1e1
J
Insl3
relative mRNA levels (normalized to Gapdh and Actb)
relative mRNA levels (normalized to Hsd3b1)
K
Intratesticular INSL3 concentration (pg/mg of tissue)
n.d
n.d.
36 dpp
D30 FT
D30 CSF
L
INSL3 concentration in medium (pg/mL)
Days of culture
FT
CSF
Basal medium

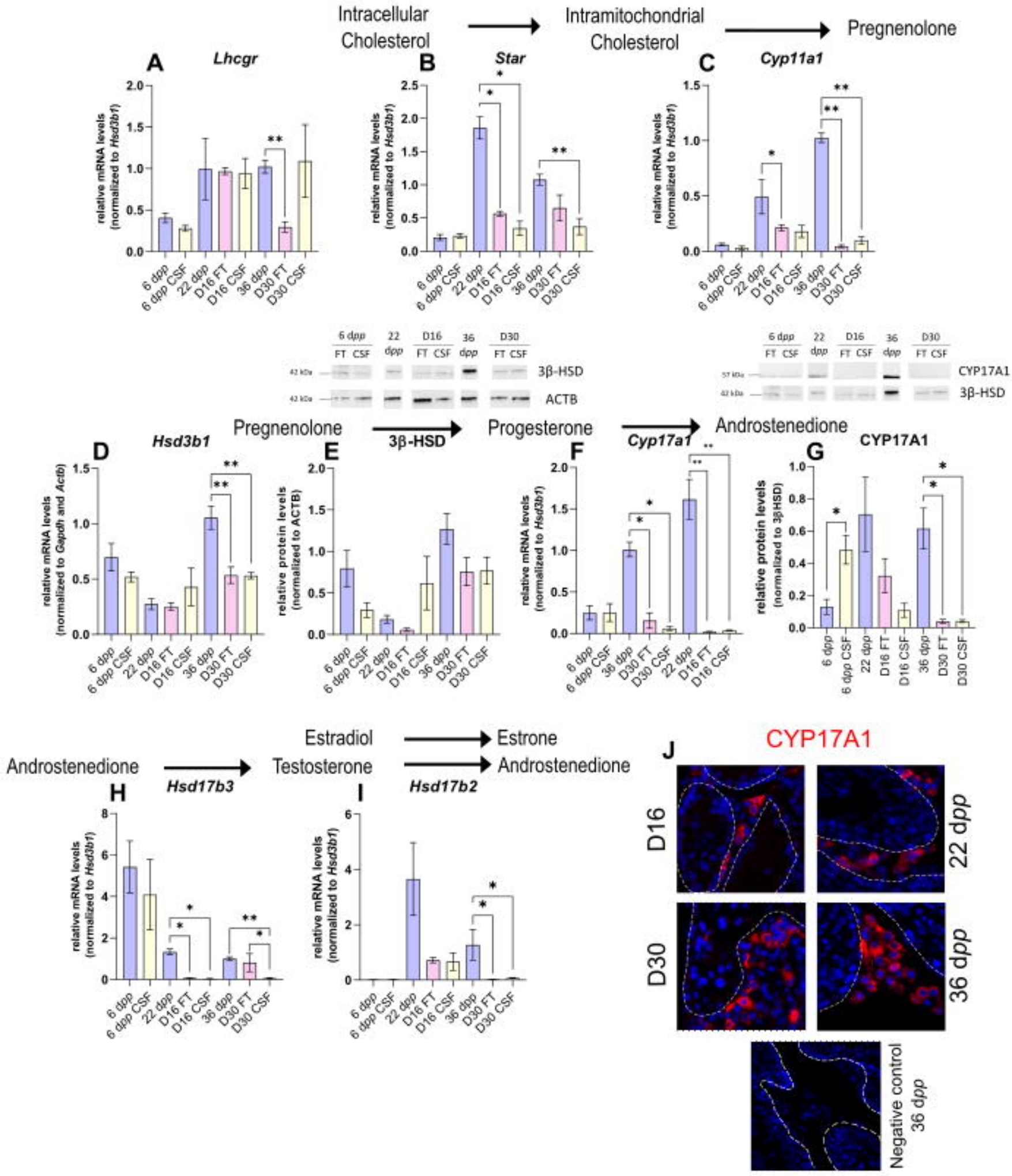
Intracellular Cholesterol
Intramitochondrial Cholesterol
Pregnenolone
A
Lhcgr
B
Star
C
Cyp11a1
relative mRNA levels (normalized to Hsd3b1)
6 dpp
6 dpp CSF
22 dpp
D16 FT
D16 CSF
36 dpp
D30 FT
D30 CSF
6 dpp
22 dpp
D16
36 dpp
D30
FT CSF
3β-HSD
ACTB
CYP17A1
Pregnenolone
3β-HSD
Progesterone
Cyp17a1
Androstenedione
D
Hsd3b1
relative mRNA levels (normalized to Gapdh and Actb)
E
relative protein levels (normalized to ACTB)
F
relative mRNA levels (normalized to Hsd3b1)
G
CYP17A1
relative protein levels (normalized to 3βHSD)
Androstenedione
Hsd17b3
Estradiol
Testosterone
Estrone
Androstenedione
Hsd17b2
H
relative mRNA levels (normalized to Hsd3b1)
I
relative mRNA levels (normalized to Hsd3b1)
J
CYP17A1
D16
D30
22 dpp
36 dpp
Negative control 36 dpp

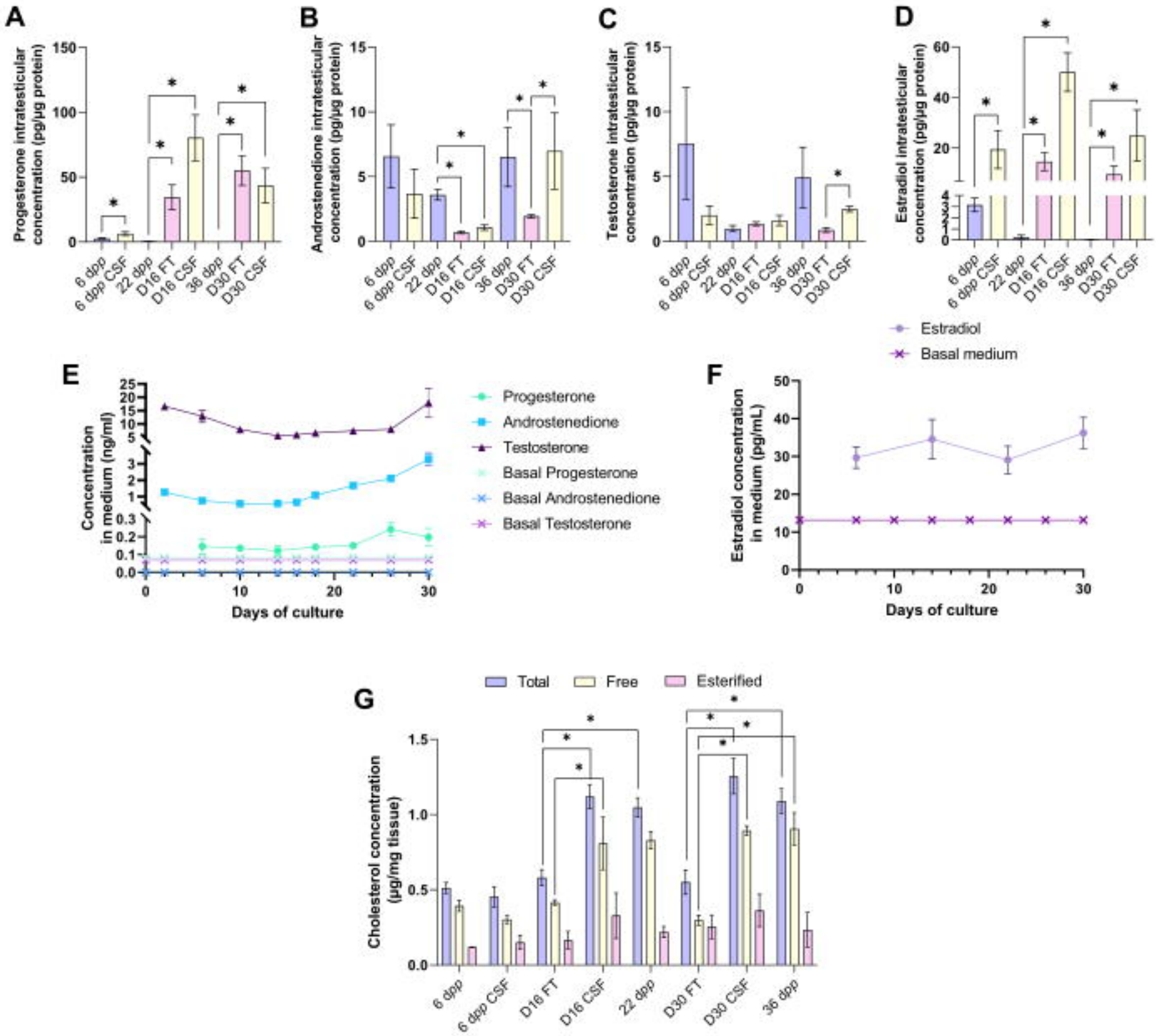
A
Progesterone intratesticular concentration (pg/µg protein)
B
Androstenedione intratesticular concentration (pg/µg protein)
C
Testosterone intratesticular concentration (pg/µg protein)
D
Estradiol intratesticular concentration (pg/µg protein)
6 dpp
6 dpp CSF
22 dpp
D16 FT
D16 CSF
36 dpp
D30 FT
D30 CSF
Estradiol
Basal medium
E
Concentration in medium (ng/ml)
Days of culture
Progesterone
Androstenedione
Testosterone
Basal Progesterone
Basal Androstenedione
Basal Testosterone
F
Estradiol concentration in medium (pg/mL)
Days of culture
G
Total
Free
Esterified
Cholesterol concentration (µg/mg tissue)

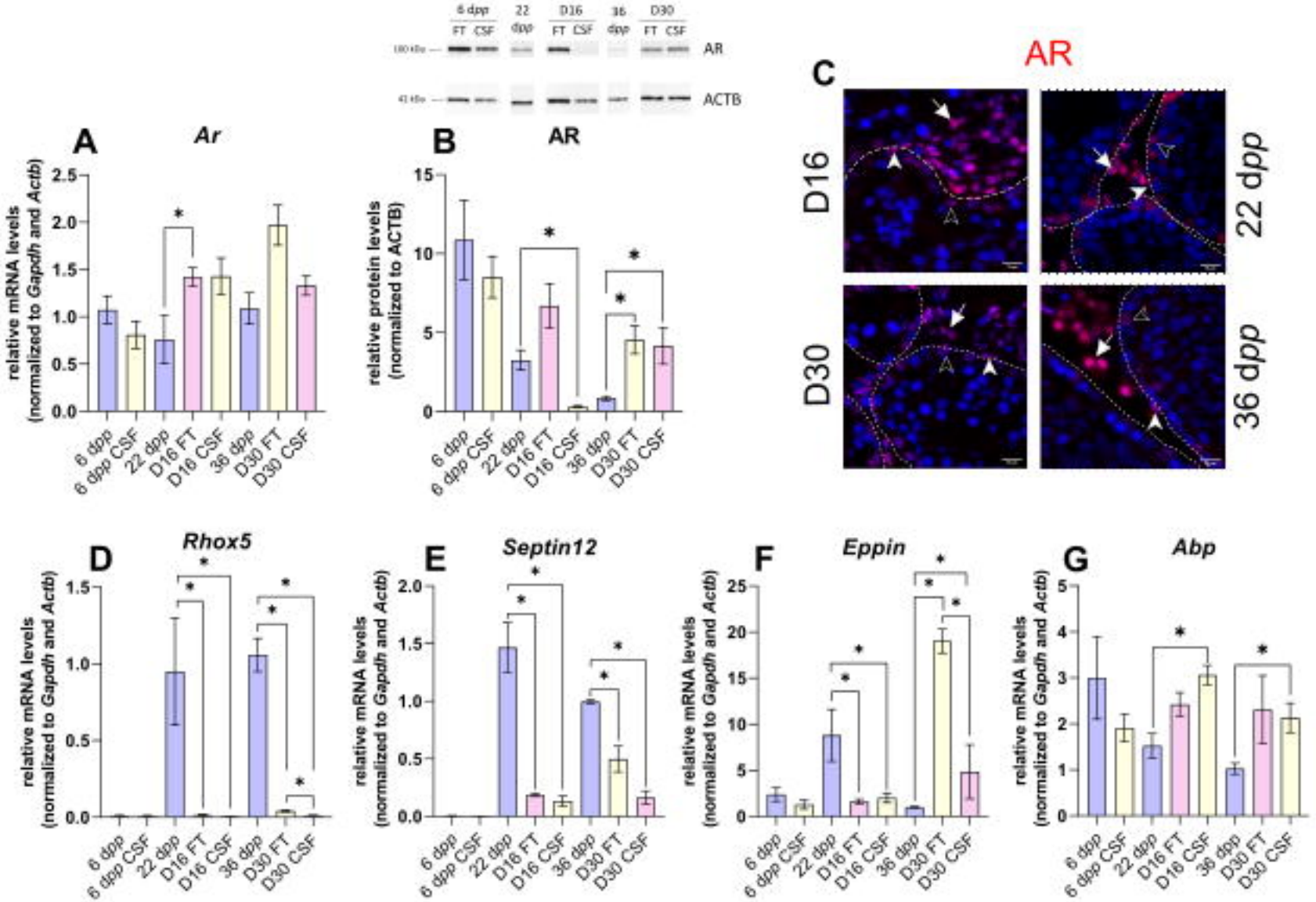
6 dpp
22 dpp
D16
36 dpp
D30
FT CSF
AR
ACTB
A
Ar
relative mRNA levels (normalized to Gapdh and Actb)
B
AR
relative protein levels (normalized to ACTB)
C
AR
D16
22 dpp
D30
36 dpp
D
Rhox5
E
Septin12
F
Eppin
G
Abp
6 dpp
6 dpp CSF
22 dpp
D16 FT
D16 CSF
36 dpp
D30 FT
D30 CSF

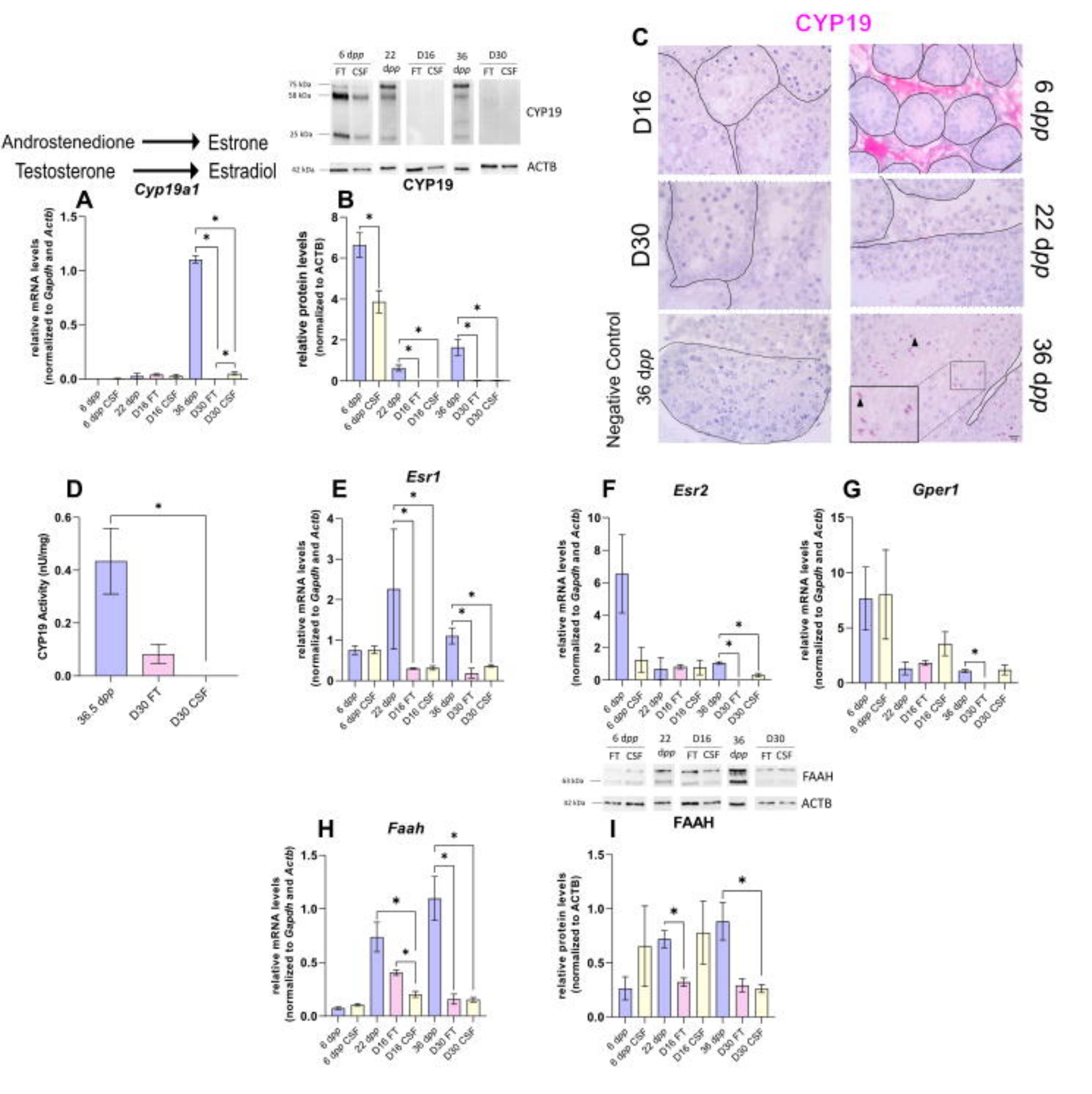
Androstenedione → Estrone
Testosterone → Estradiol
Cyp19a1
A
relative mRNA levels (normalized to Gapdh and Actb)
6 dpp
6 dpp CSF
22 dpp
D16 FT
D16 CSF
36 dpp
D30 FT
D30 CSF
6 dpp
22 dpp
D16
36 dpp
D30
FT CSF
75 kDa
58 kDa
25 kDa
CYP19
42 kDa
ACTB
CYP19
B
relative protein levels (normalized to ACTB)
C
CYP19
D16
D30
36 dpp
Negative Control
6 dpp
22 dpp
36 dpp
D
CYP19 Activity (nU/mg)
36.5 dpp
D30 FT
D30 CSF
E
Esr1
F
Esr2
G
Gper1
FAAH
ACTB
H
Faah
I
FAAH

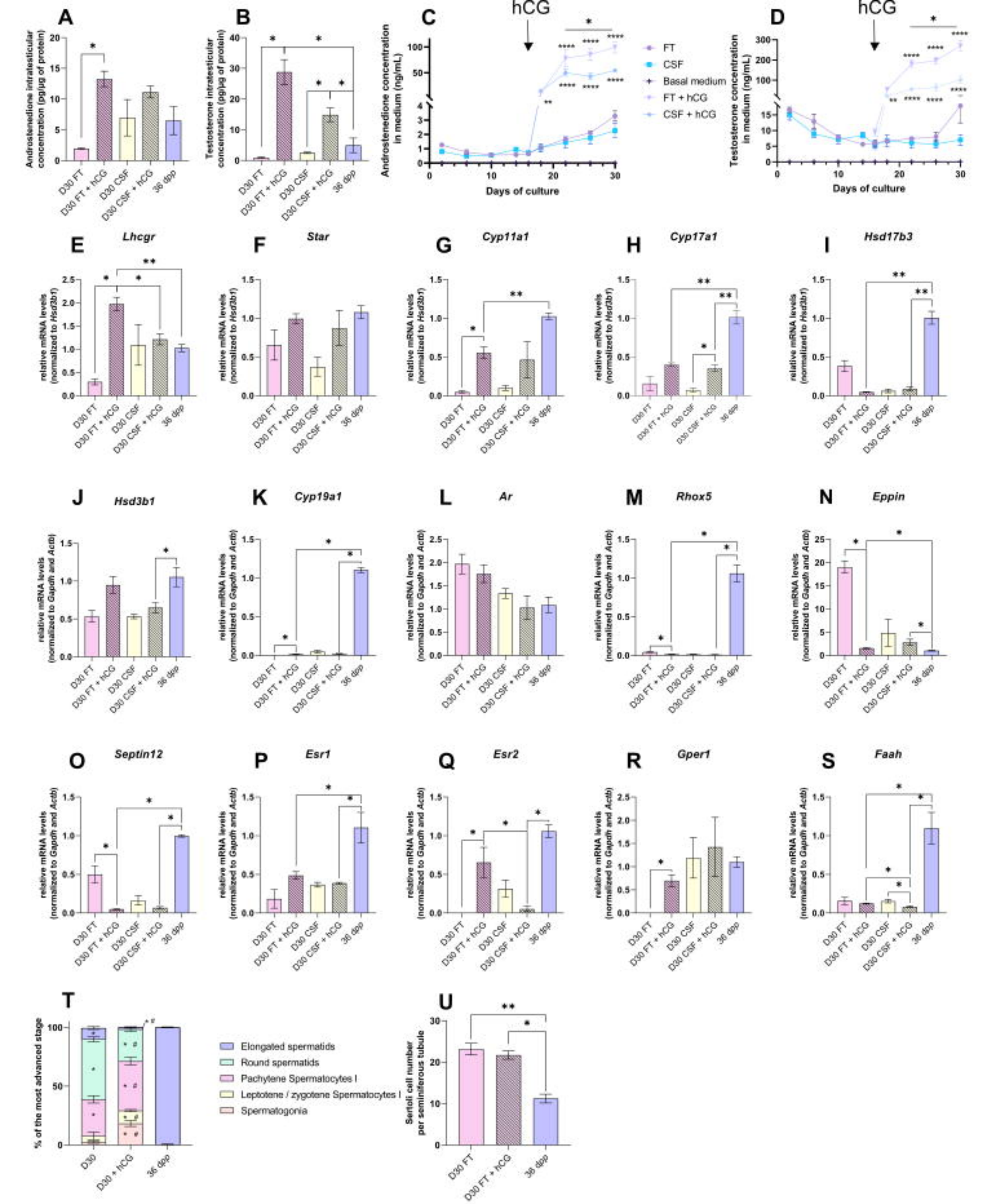
A
Androstenedione intratesticular concentration (pg/µg of protein)
B
Testosterone intratesticular concentration (pg/µg of protein)
C
hCG
Androstenedione concentration in medium (ng/mL)
Days of culture
FT
CSF
Basal medium
FT + hCG
CSF + hCG
D
hCG
Testosterone concentration in medium (ng/mL)
Days of culture
D30 FT
D30 FT + hCG
D30 CSF
D30 CSF + hCG
36 dpp
E Lhcgr
F Star
G Cyp11a1
H Cyp17a1
I Hsd17b3
J Hsd3b1
K Cyp19a1
L Ar
M Rhox5
N Eppin
O Septin12
P Esr1
Q Esr2
R Gper1
S Faah
relative mRNA levels (normalized to Hsd3b1)
relative mRNA levels (normalized to Gapdh and Actb)
T
% of the most advanced stage
D30
D30 + hCG
36 dpp
Elongated spermatids
Round spermatids
Pachytene Spermatocytes I
Leptotene / zygotene Spermatocytes I
Spermatogonia
U
Sertoli cell number per seminiferous tubule

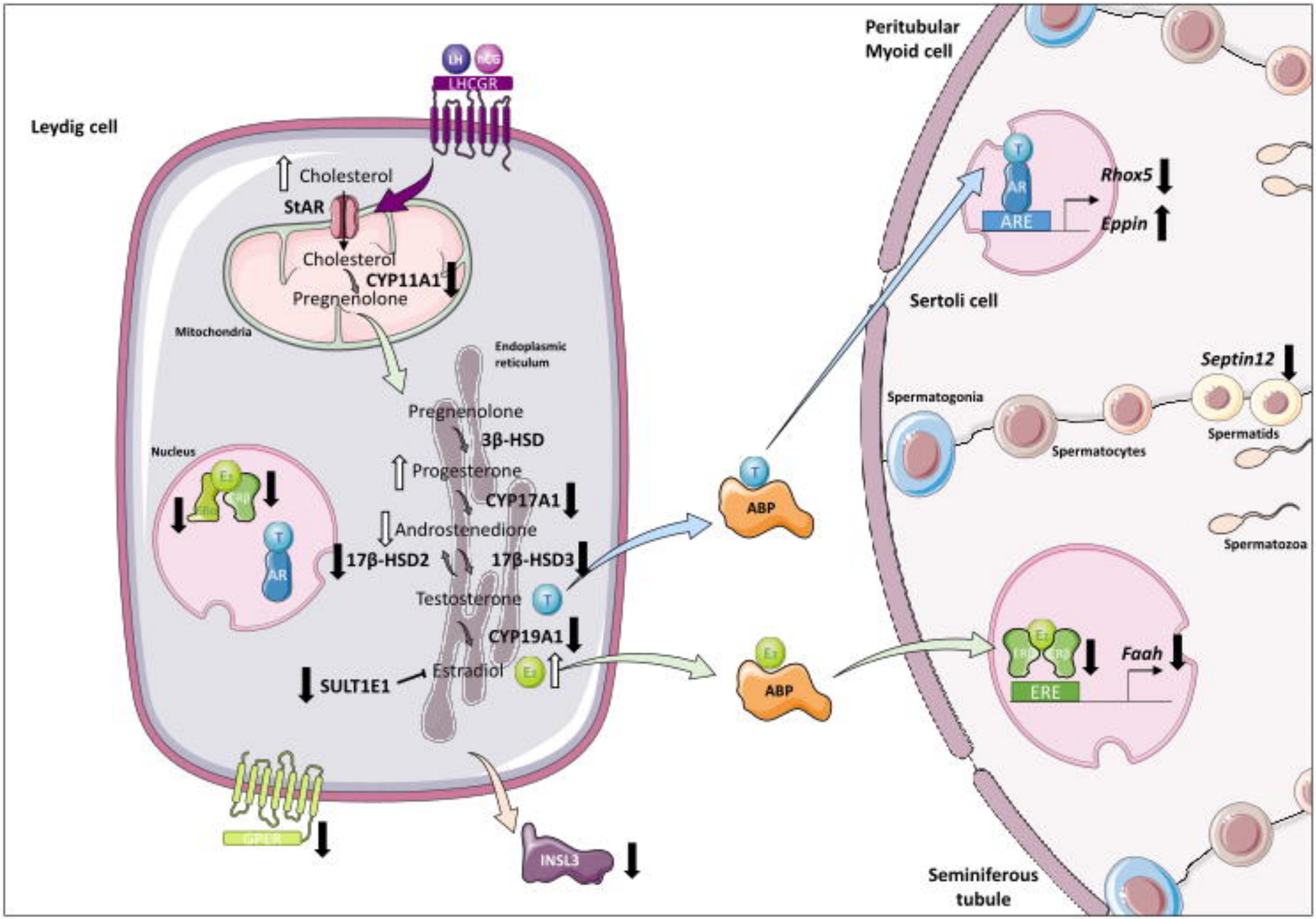
Leydig cell
LH
hCG
LHCGR
Cholesterol
StAR
Cholesterol
CYP11A1
Pregnenolone
Mitochondria
Endoplasmic reticulum
Pregnenolone
3β-HSD
Progesterone
CYP17A1
Androstenedione
17β-HSD2
17β-HSD3
Testosterone
CYP19A1
SULT1E1
Estradiol
Nucleus
T
AR
GPER
INSL3
ABP
ABP
Peritubular Myoid cell
T
AR
ARE
Rhox5
Eppin
Sertoli cell
Septin12
Spermatogonia
Spermatocytes
Spermatids
Spermatozoa
ERE
Faah
Seminiferous tubule

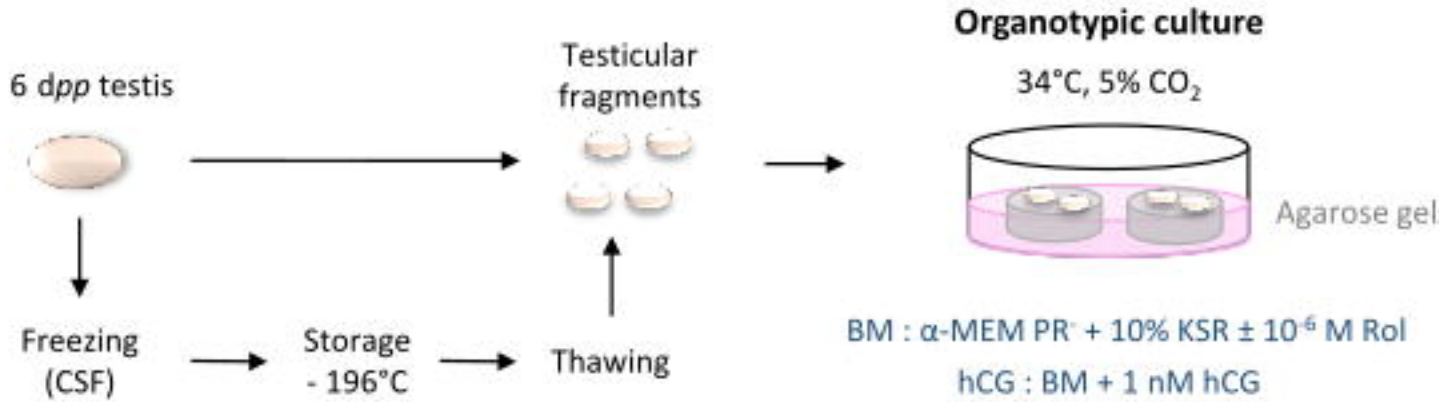
6 dpp testis
Testicular fragments
Organotypic culture
34°C, 5% CO_2
Agarose gels
Freezing (CSF)
Storage - 196°C
Thawing
BM : α-MEM PR⁻ + 10% KSR ± 10^{-6} M RoI
hCG : BM + 1 nM hCG

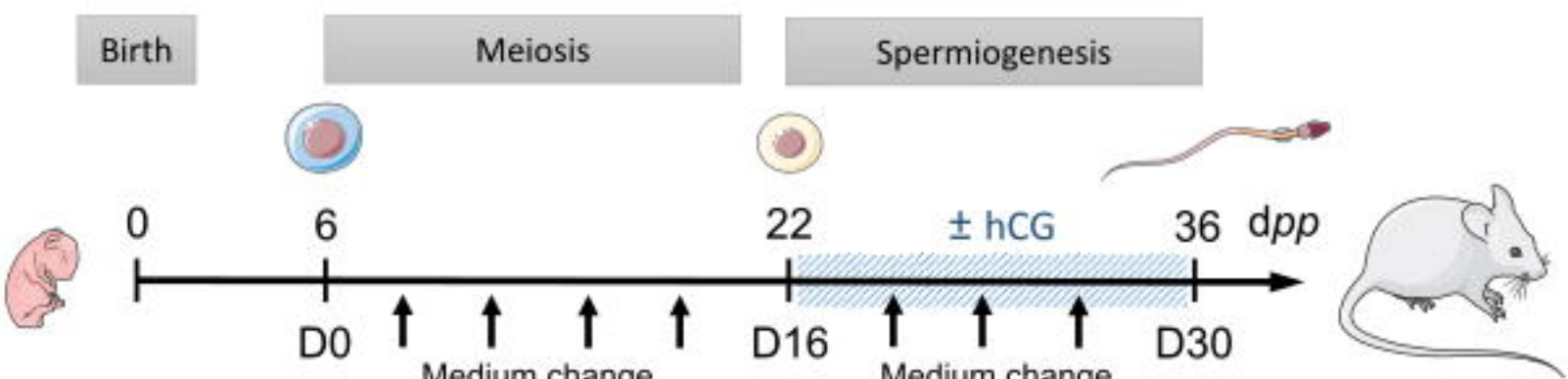
Birth
Meiosis
Spermiogenesis
0
6
22
± hCG
36
dpp
D0
D16
D30
Medium change
Medium change